IFNAR1 controls risk of Cerebral Malaria in children and mediates brain pathology by $CD8^+$ T cells in *P.berghei*-infected mice.

Elizabeth A. Ball[1], Maria Rosário Sambo[1, 2, 3] , Madalena Martins[1,4],
Maria Jesus Trovoada[1, 5], Carla Benchimol[3], João Costa[1], Lígia A. Gonçalves[1],
António Coutinho[1], Carlos Penha-Gonçalves[1]

Author affiliations

[1]Instituto Gulbenkian de Ciência, 2781-901 Oeiras, Portugal;
[2]Faculdade de Medicina, Universidade Agostinho Neto, Luanda, Angola;
[3] Hospital Pediátrico David Bernardino, Luanda, Angola;
[4]Neurological Clinical Research Unit, Instituto de Medicina Molecular, Faculdade de Medicina da Universidade de Lisboa, 1649-028 Lisboa, Portugal;
[5]Centro National de Endemias, São Tomé and Príncipe;

Corresponding author

Carlos Penha Gonçalves, Rua da Quinta Grande, 6, 2780 Oeiras, Portugal,
00351 214464634
cpenha@igc.gulbenkian.pt

Running Title

Resistance to cerebral malaria by IFNAR1.

Total number of characters without spaces

30,455

Key words

$CD8^+$ T cells, Cerebral malaria, Experimental Cerebral malaria, Genetic association, *IFNAR1*

Abbreviations

CM, Cerebral malaria; ECM, Experimental cerebral malaria; *IFNAR1*, Interferon alpha/beta receptor 1; iRBC, infected red blood cell; *PbA*, *Plasmodium berghei* ANKA-GFP; SNP, Single Nucleotide Polymorphism; UIF, Uninfected controls; UM, Uncomplicated malaria;

Abstract

Development of cerebral malaria (CM), a severe form of clinical *Plasmodium falciparum* infection results from brain injury involving a damaging cascade of vascular, inflammatory and immunological events. Susceptibility to CM is modified by host genetic factors and our case-control study in Angolan children aimed at highlighting genes implicated in progression to CM. We report here on one candidate gene found, *IFNAR1,* which carries a haplotype consisting of eight single nucleotide polymorphisms (SNPs) that conferred increased risk in acquiring malaria infection but protected against progression to CM. Equal protection from Experimental (E) CM was found in *Ifnar1-/-* mice infected with *Plasmodium berghei* ANKA. Generating a novel transfer protocol that initiates spleen cell priming, we identified the crucial need of IFNAR1 within $CD8^+$ T cells to abrogate resistance to ECM in *Ifnar1-/-* mice. Splenic $CD8^+$ T cells from *Ifnar1-/-* mice showed a cytotoxic profile upon infection yet were unable to mediate ECM development within the brain tissue. This shows that IFNAR1 signaling is critical in $CD8^+$ T cells to unfold their pathogenic role. Our cohesive findings between human and mouse studies thus demonstrates that IFN-I responses through IFNAR1 are vital components in CM pathogenesis.

Introduction

Cerebral malaria (CM) is a severe complicated form of *Plasmodium falciparum* malaria, affecting mostly children in endemic regions (Issifou et al., 2007; Mackintosh et al., 2004; Newton and Krishna, 1998). Adhesion and sequestration of infected red blood cells (iRBCs) in brain microvasculature leading to blood vessel occlusion is central to CM pathogenesis (Milner, 2010) but immunological mechanisms operating during development of CM remain unclear.

Research into understanding the progression and control of CM development in humans is hindered by limited accessibility to human tissues (Carvalho, 2010). Therefore usage of the mouse model, termed Experimental Cerebral Malaria (ECM) has enabled research to uncover cellular and molecular components in CM. The relevance of mouse ECM was recently addressed and emphasized the need of denoting consistent factors between the human and mouse model (Craig et al., 2012; de Souza et al., 2010; Renia et al., 2010; Riley et al., 2010). As such factors are seldom confirmed, confounding lists of players in CM development has emerged as a result. One factor however remaining implicit are $CD8^+$ T cells (Belnoue et al., 2002; Hermsen et al., 1997) although the exact mechanisms that drive $CD8^+$ T cell pathogenesis in CM remain unclear to this day.

The role of cytokines in human CM development has been brought to light in recent genetic studies (reviewed by (Driss et al., 2011). Initial reports by (Aucan et al., 2003; Khor et al., 2007) began exploring the necessary role of Type I interferons (IFN-I) and CM progression, showing that genetic polymorphisms in the interferon type 1 receptor (*IFNAR1*) led to protection from CM development. As IFNAR1 is the key signaling receptor needed for IFN-I activity (Diop et al., 2006) and is expressed on virtually every cell surface (Ito et al., 2006; Prinz et al., 2008) the impact IFN-I has on the immune response is vast. Recent publications addressedIFN-I actions dictated through the IFNAR1 receptor in response to hemozoin derivatives (Sharma et al., 2011) and in controlling parasite burden (Haque et al., 2011a) upon *Plasmodium* infection. IFN-I has also been shown to be involved in the priming of $CD8^+$ T cells (deWalick et al., 2007; Lundie et al., 2008) and in the generation of a robust immune response to infection (Huys et al., 2009). However the exact caliber of *IFNAR1* actions in CM development is still unexplored.

Correlations with *IFNAR1* and CM in human genetic studies have been reported (Aucan et al., 2003; Khor et al., 2007). We performed a genetic study designed to compare specifically uncomplicated malaria (UM) and CM patients in order to generate gene candidates involved in CM progression. We selected children, the primary severe malaria risk group, from an area of Angola where malaria transmission is perennial (e Pinto and Alves, 2008). We further identified *IFNAR1* as a candidate gene. This drove us to use the *Ifnar1-/-* mouse model to uncover its exact involvement. We found that *Ifnar1-/-* mice are equally protected from ECM and by developing a novel transfer protocol we exposed the necessity of IFN-I in $CD8^+$ T cell immune responses during *Plasmodium* infection.

Results

IFNAR1 variants are associated with protection against clinical progression to cerebral malaria.

The *IFNAR1* gene has been associated to severe forms of malaria (Aucan et al., 2003; Khor et al., 2007). Here we made use of a cohort of Angolan children to identify *IFNAR1* genetic variants that specifically modify the risk of progressing to CM syndrome from uncomplicated forms of malaria. We compared single nucleotide polymorphisms (SNPs) allelic frequencies in infected children that developed CM (n = 110) with children that only manifested clinically uncomplicated malaria (UM) (n = 129). We analyzed UM patients against uninfected (UIF) controls (n = 305) to ascertain whether *IFNAR1* gene polymorphisms were involved in susceptibility to malaria in this sample collection (Table S1). Eight out of 18 *IFNAR1* SNPs showed suggestive association ($P < 0.05$) both with malaria susceptibility and with progression to CM (Fig. 1b) (Table S2) possibly under a dominant mode of action (Table S3). The two markers having the strongest association, both with UM risk and with progression to CM, rs2856968 (P = 2.36E−5 and P = 6.15E−5, respectively) rs2253923 (P = 2.50E−3 and P = 5.00E−4, respectively) remained significantly associated after conservative Bonferroni correction for multiple testing (P < 2.78E−3) (Fig. 1b). Genotypic association under the dominant model essentially confirms the results obtained for the allelic association (Table S3). Strikingly, the genetic effect analysis indicates that minor frequency alleles at these markers conferred increased risk of acquiring UM (rs2856968: $OR_G = 2.00$, rs2253923: $OR_T = 1.61$) but protected from progression to CM syndrome (rs2856968: $OR_G = 0.42$, rs2253923: $OR_T = 0.49$) (Fig. 1c, Table S2). These two SNPs are in strong linkage disequilibrium (LD)

($r^2 = 0.77$) suggesting that the observed associations may represent a single causal genetic variant (Fig. 1d).

Haplotypic association analysis comprising eight SNPs in the 5' *IFNAR1* gene region (encompassing upstream regulatory region, intron 1 and intron 2) identified one reconstructed haplotype (GGGGTGCT) showing robust association with UM susceptibility ($P_{hap} = 1.22E{-}5$; $OR_{hap} = 2.02$) and with protection against progression to CM ($P_{hap} = 6.89E{-}7$; $OR_{hap} = 0.34$) (Table 1). Conversely, the most frequent haplotype for the same eight SNPs (ACAACGCA) evidenced an opposite effect by conferring protection against mild malaria ($P_{hap} = 1.20E{-}3$; $OR_{hap} = 0.62$) while increasing the risk of progression to CM ($P_{hap} = 8.0E{-}4$; $OR_{hap} = 1.87$). Together this genetic evidence strongly suggests that *IFNAR1* gene variants that increase the risk of acquiring UM also provide protection against CM. This proposes a dual role of *IFNAR1* during the inflammatory response to malaria infection and at principally dictating progression to CM.

***Ifnar1-/-* mice are protected from development of Experimental Cerebral Malaria and brain pathology.**

To ascertain whether *IFNAR1* is involved in inflammation evoked by malaria infection we used the mouse model of ECM which mainly results from exacerbated inflammatory responses in the brain tissue (Craig et al., 2012). In line with a recent report (Sharma et al., 2011) we observed that *P.berghei* ANKA GFP (*PbA*) infection in *Ifnar1-/-* mice led to strong resistance to ECM (75% ECM resistance, Fig. 2a) in comparison to susceptible C57BL/6 control mice. Surviving *Ifnar1-/-* mice die between days 25-30 from anemia and hyperparasitemia, without displaying signs of ECM development and showed parasitemia comparable to C57BL/6 mice in the period that preceded ECM death, up to day 6 PI (Fig. 2b). This indicates that ECM resistance in *Ifnar1-/-* mice was not related to decreased peripheral parasite burden.

A standard hallmark in ECM is destruction of the blood brain barrier (BBB) (Ferreira et al., 2011). We analyzed infected and non-infected C57BL/6, *Ifnar1-/-* as well as ECM resistant BALB/c mice for barrier breakage using Evans blue perfusion. Our results revealed that alike BALB/c mice, *Ifnar1-/-* mice display no BBB breakage (Fig. 3a and b) as opposed to C57BL/6 mice that showed abundant dye leakage in the brain. Histopathological analysis of infected C57BL/6 brain sections exhibited prominent mononuclear cell accumulations within brain microvessels (Fig. 3d) with evidence of disruption of vessel walls and endothelial cell destruction (Fig. 3e). Parenchymal hemorrhagic lesions in C57BL/6 infected mice were observed, containing infected red blood cells (iRBCs) (Fig. 3f). *Ifnar1-/-* mice in contrast displayed mild intravascular accumulation of mononuclear cells (Fig. 3h) within brain blood vessels and showed endothelial cells unaffected (Fig. 3i). Hemorrhagic lesions were absent in *Ifnar1-/-* mice sections and iRBCs were seen within the lumen of the blood vessels only (Fig. 3j). These results show that despite abnormal mononuclear accumulation within brain microvessels and presence of intraluminal iRBCs, infected *Ifnar1-/-* mice do not show typical pathology of ECM.

Ifnar1-/- **mice display a delayed inflammatory response upon infection, in brain tissue.**

To further investigate the mechanisms underlying protection of *Ifnar1-/-* infected mice against brain pathology we evaluated the parasite burden in the brain of C57BL/6 and *Ifnar1-/-* infected mice. Quantification of *P. berghei* rRNA showed no significant differences during the early time course of infection, strongly suggesting that ECM protection in *Ifnar1-/-* mice was not attributable to reduced brain parasite burden (Fig. 4a). We also observed that kinetics of *Cd3* mRNA expression in the brain leading up to ECM manifestations was slightly lower in *Ifnar1-/-* mice but not significantly different from C57BL/6 mice, suggesting that T cell migration to the brain during infection was not impaired in *Ifnar1-/-* mice (Fig. 4b). Nevertheless, we found that in the brain of *Ifnar1-/-* mice the expression of inflammatory markers, namely *Tnf-alpha* and *Il10* had significantly lower induction in the period preceding ECM onset and showed delayed kinetics as compared to C57BL/6 infected mice. Overall, these results indicate that in spite the accumulation of iRBCs and presence of T cells, *Ifnar1-/-* mice unfold a diminished exacerbation in inflammatory responses deterring the development of brain pathology within the time window of ECM development upon *PbA* infection.

C57BL/6 spleen cells confer ECM susceptibility to *Ifnar1-/-* mice

We then questioned in which cell type lack of IFNAR1 was fundamental in protecting mice from ECM development. We developed a novel transfer protocol to assess individual cell type ability at restoring ECM susceptibility in *Ifnar1-/-* mice (Fig. 5a). Cells from donor mice are primed *in vivo* to parasite antigens by exposure to irradiated iRBC. The irradiated parasite being now unable to re-invade RBC, ceases infection at this stage and cell donor C57BL/6 mice do not develop parasitemia or ECM (data not shown). A group of C57BL/6 cell donor mice were injected with irradiated iRBC and then infected with 1×10^6 non-irradiated *PbA* iRBC 7 days later, as per normal infection. All mice subsequently developed ECM and died by day 7 PI (data not shown). Therefore we concluded that our protocol is not an immunization but rather a pre-sensitization protocol, in absence of parasite development.

We used this protocol to assess whether total splenocytes from C57BL/6 mice could induce ECM in the resistant *Ifnar1-/-* strain. Total splenocytes were transferred from C57BL/6 cell donor mice that had received non-infected irradiated RBC to *Ifnar1-/-* recipient mice. When infected 1 hour post-transfer *Ifnar1-/-* recipient mice developed parasitemia alike *Ifnar1-/-* mice that received no cell transfer and infection only. Neither group of mice developed ECM with all mice dying around day 25 PI from anemia and hyperparasitemia (Fig. 5b). This shows that naïve C57BL/6 splenocytes are unable to induce ECM susceptibility in *Ifnar1-/-* mice. Total splenocytes were then transferred from C57BL/6 cell donors that had received irradiated iRBC, to *Ifnar1-/-* mice. The infected recipient *Ifnar1-/-* mice showed 75% development of ECM within the period of 6-12 days PI when control C57BL/6 mice develop disease (Fig. 5c). This demonstrates that C57BL/6 splenocytes pre-sensitized to irradiated iRBC are effective at restoring ECM susceptibility in *Ifnar1-/-* mice.

We then aimed to determine whether $CD8^+$ cells within total spleen cells were inducing ECM in *Ifnar1-/-* mice. Sorted $CD8^+$ or CD8-depleted cells were transferred from C57BL/6 cell donor mice that had received irradiated iRBC into recipient *Ifnar1-/-* mice. Recipients were then infected 1 hour after transfer. Levels of parasitemia did not differ between the two groups of mice when compared against *Ifnar1-/-* mice that received no cell transfer and infection only (Fig. 5d). In contrast, we found ECM development in only the group of *Ifnar1-/-* mice that received purified $CD8^+$ cells, indicating that pre-sensitized C57BL/6 $CD8^+$ cells were able to restore susceptibility to ECM in *Ifnar1-/-* mice (Fig. 5e). We confirmed the ability of pre-sensitized $CD8^+$ cells isolated from C57BL/6 mice at inducing *bone fide* ECM by assessing BBB integrity. BBB breakage was observed in recipient *Ifnar1-/-* mice that received C57BL/6 $CD8^+$ cells and not in recipients of CD8-depleted cells (Fig. 5f-g).

Together these results expressly show that IFNAR1 is critical for abrogation of ECM resistance mediated by pre-sensitized CD8$^+$ cells in *Ifnar1-/-* mice.

Intrinsic CD8$^+$ T cell properties trigger ECM development.

In order to ascertain dependency of ECM induction on IFNAR1 expression in CD8$^+$ cells we modified our cell transfer protocol (Fig. 6a). CD8$^+$ cells were sorted from *Ifnar1-/-*.Ly5.2 non-infected mice and transferred to previously non-lethally irradiated C57BL/6.Ly5.1 mice, allowing discrimination of endogenous and transferred CD8$^+$ populations. Ly5.1/5.2 chimeric mice then received irradiated iRBCs from a B6.Ly5.1 mouse. Seven days after Ly5.1 CD8$^+$ and Ly5.2 CD8$^+$ cell populations were sorted (Fig. 6b) and transferred to *Ifnar1-/-* recipient mice. No differences in parasitemia progression were observed in either group as compared to *Ifnar1-/-* mice that received no cell transfer and infection only (Fig. 6c). Conclusively we found that only recipient *Ifnar1-/-* mice that had received Ly5.1 IFNAR1$^+$ CD8$^+$ cells developed ECM, showing 100% disease incidence while recipients of Ly5.2 IFNAR1$^-$ CD8$^+$ cells maintained their high degree of ECM resistance comparable to *Ifnar1-/-* mice that received no cell transfer and infection only. This demonstrates that expression of IFNAR1 in CD8$^+$ cells is required to terminate ECM resistance in *Ifnar1-/-* mice. This strongly suggests that deficiency in IFNAR1 signaling in CD8$^+$ T cells impairs their ability to induce ECM in *Ifnar1-/-* mice during *PbA* infection.

***Ifnar1-/-* mice display differing activation states in spleen and brain tissue compared to C57BL/6 mice.**

To investigate CD8$^+$ T cell impairments in *Ifnar1-/-* mice during *Pb*A infection we analyzed the activation and expansion of CD8$^+$ T cells in the spleen at day 5 PI, prior to ECM onset. We found a significant difference between non-infected C57BL/6 and *Ifnar1-/-* mice, which was attenuated upon infection. This indicates that infection-driven $CD8^+$ T cell expansion was not impaired in *Ifnar1-/-* mice (Fig. 7a). Similarly, splenic $CD8^+$ T cells from *Ifnar1-/-* mice did not show impairments in intracellular up-regulation of Granzyme B (GrB) or Interferon gamma (IFN-γ) upon infection (Fig. 7b and c).

Likewise, we analyzed profiles of $CD8^+$ T cells from the brain of C57BL/6 and *Ifnar1-/-* infected mice at day 6 PI, upon display of end stage ECM symptoms in C57BL/6 mice. We found that total number of $CD8^+$ T cells sequestered in the brain of *Ifnar1-/-* mice was significantly reduced compared to C57BL/6 mice (Fig. 7d). Nevertheless, the vast majority of brain sequestered $CD8^+$ T cells in both *Ifnar1-/-* and C57BL/6 mice were activated and showed a cytotoxic profile (Fig. 7e and f). This indicated no faltering in sequestered *Ifnar1-/-* $CD8^+$ T cells to exhibit a cytotoxic profile. Analysis of mean fluorescence intensity of GrB+ and IFN-γ+ in $CD8^+$ T cells from infected mice corroborates the notion that accumulated *Ifnar1-/-* $CD8^+$ T cells have no faltering in exhibiting a cytotoxic profile. (Fig. S2).

We confirmed these results by analyzing sequestered $CD8^+$ T cells, day 6 PI, from ECM restored *Ifnar1-/-* mice compared against *Ifnar1-/-* mice that received CD8-depleted cells. As expected, we found that the number of $CD8^+$ T cells sequestered in the brain as well as the number of GrB+ IFN-γ+ $CD8^+$ T cells was higher in mice that received $CD8^+$ T cells when compared to mice that received CD8-depleted cells (Fig. 7g-i). This suggests that induction of ECM in these mice is a result of increased sequestration of activated cytotoxic $CD8^+$ T cells. Our data indicates that activation of $CD8^+$ T cells in *Ifnar1-/-* mice do not show impaired activation and, although at reduced numbers in the brain, *Ifnar1-/-* mice definitely sequester activated $CD8^+$ T cells.

Discussion

This work uncovers pleiotrophic effects of Type I interferons/*IFNAR1* signaling system during malaria infection in humans and mice. Two previous reports described genetic association of *IFNAR1* with susceptibility to severe malaria (Aucan et al., 2003; Khor et al., 2007). Nevertheless we found that *IFNAR1* genetic variants that increased the risk of UM in Angolan children also showed protection against progression to CM. Our findings imply a dual role of *IFNAR1* genetic variants in controlling the clinical outcome of malaria infection, a finding not discernible from the previously reported comparisons.

In Gambian children, two SNPs were identified in the *IFNAR1* gene in intron 3 and exon 4 that were associated with severe malaria and CM cases (Aucan et al., 2003). However the study embarking Gambian, Kenyan and Vietnamese populations (Khor et al., 2007) highlighted positive associations in the 5' region of the *IFNAR1* locus. This was also found as a region of strong association in our study of Angolan children suggesting that this locus represents a widespread malaria susceptibility factor. Furthermore, the design established in our study proved to be advantageous, allowing us to specifically evaluate the association of *IFNAR1* with disease risk (to CM or UM) and with disease progression in severity (from UM to CM). Our results illustrate the diverse role of an IFN-I response during different clinical forms of *Plasmodium* infection. *IFNAR1* variants have also been associated with AIDS progression (Diop et al., 2006) and with the clinical presentation of hepatitis B virus infection (Song le et al., 2008) allowing the inference that *IFNAR1* variants impact on IFN-I responses governing the clinical course and progression in different infectious diseases.

These results implicating *IFNAR1* in human CM protection motivated the use of *Ifnar1-/-* mice to exploit the mechanisms of CM development in the ECM mouse model. We found that protection from ECM in *Ifnar1-/-* mice was not controlled via parasite burden, concluding that IFN-I mechanisms were dominant during other stages of ECM pathogenesis. *Ifnar1-/-* mice developed a rapid and steep rate of parasitemia throughout the course of infection and in addition, parasite accumulated within the brain tissue at comparable levels to susceptible C57BL/6 mice. In contrast IFN-I dependent mechanisms have implicated $CD4^+$ T cells in controlling *PbA* parasitemia through undefined cell types (Haque et al., 2011a). However increasing parasite burden during infection in *Ifnar1-/-* mice was not sufficient enough at provoking an inflammatory response leading to BBB breakage or at inducing accumulation of mononuclear cells within brain micro-vessels.

The development of a novel transfer protocol allowed focus on cellular mechanisms involved in ECM protection conferred by IFNAR1. These experiments uncovered that IFNAR1 in primed splenic $CD8^+$ cells is unequivocally needed to abrogate ECM resistance in *Ifnar1-/-* mice. Further, cell transfers of cytotoxic $CD8^+$ T cells have shown ECM induction in perforin (Nitcheu et al., 2003) and Granzyme B-deficient mice (Haque et al., 2011b), demonstrating that a $CD8^+$ T cell cytotoxic profile is needed in ECM development. It has however never been contextualized exactly what mechanism within the spleen drives $CD8^+$ cytotoxic ability during ECM development. No hindrances in the cytotoxic profile of splenic *Ifnar1-/-* $CD8^+$ T cells were observed upon infection (Fig. 7a-c) suggesting that priming in the spleen is not impaired. Nevertheless we cannot exclude that IFN-I/IFNAR1 signaling system represent as ancillary mechanism in priming $CD8^+$ T cells specific for *Plasmodium* antigens, which is unavailable in *Ifnar1-/-* mice.

On the other hand we observed that *Ifnar1-/-* ECM resistant mice retained lower numbers of activated $CD8^+$ T cells in the brain, suggesting that IFN-I influences ECM susceptibility within the brain tissue. Inflammatory stimuli, specifically IFN-I have been shown as critical in maintaining $CD8^+$ T cells at their site of effector function (Marrack et al., 1999). This hints that unresponsive *Ifnar1-/-* $CD8^+$ T cells have impaired ability to accumulate within the brain tissue. Moreover, we noted that *Ifnar1-/-* mice receiving C57BL/6 primed $CD8^+$ splenocytes accumulated relatively low numbers of activated $CD8^+$ T cells within the brain tissue, yet developed ECM (Fig. 7g-i). This provokes the notion that induction of ECM in transferred mice was not due to $CD8^+$ T cell accumulation but was evoked by low numbers of $IFNAR1^+$ $CD8^+$ T cells. In fact *Ifnar1-/-* mice appear to be capable in generating a cytotoxic profile (Fig. S2) but their cytotoxic effector capacity could be impaired (Le Bon et al., 2006) leading to hindrances in their ECM pathogenesis.

Evidence has shown that $CD8^+$ T cells need constant stimulation via antigen presentation to remain at their effector site (Galea et al., 2007; Miu et al., 2008; Stewart, 2003). Inability of *Ifnar1-/-* $CD8^+$ T cells to induce ECM appears to be due to their unresponsiveness to IFN-I signals in the context of antigen presentation within the brain tissue. Potential sources of such signals include professional antigen presenting cells (APC) or endothelial cells (EC) (Combes et al., 2010). Moreover, EC could act as an APC to present parasite antigens as well as providing co-stimulatory signals to $CD8^+$ T cells (Razakandrainibe et al., 2012). Research has shown that IFN-I can act as a licensing signal for APCs (Hervas-Stubbs et al., 2011; Kolumam et al., 2005). However, the exact nature of how $CD8^+$ T cells are presented in the brain is not known. We hypothesize that IFNAR1 impacts upon $CD8^+$ T cells stimulation at different stages of malaria infection. We suggest the spleen as a primary site of parasite antigen presentation and propose that a secondary site of stimulation and presentation to $CD8^+$ T cells occurs within the brain tissue.

The collective work presented here shows the cohesive role of *IFNAR1* during CM development in both conferring human CM protection and as an implicator of $CD8^+$ T cell pathology in mouse ECM. Together these results classify IFN-I responses through IFNAR1 as vital components in CM pathogenesis and validate the mouse model in understanding IFNAR1 involvement in CM pathology.

Material and Methods

Patient and control samples

A total of 591 children, living in Luanda and ranging from 6 months to 13 years of age were enrolled in the present study. Ethical permission for this study was granted by the Ethical Committee of the Hospital Pediátrico David Bernardino (HPDB) in Luanda, appointed by the Angolan Ministry of Health. Written, informed consent was obtained from the parents or guardians of each child. Patients were selected from attendees to the HPDB. UIF controls were sampled from children randomly selected from the vaccination ward of the HPDB. The details of the dataset have been described previously (Sambo et al., 2010). Briefly, samples were collected from children aged 6-159 months, carried out between February 2005 to May 2007 and comprised of 130 patients with CM, 142 patients with UM and 319 children as UIF controls. Malaria was diagnosed on the basis of a positive asexual parasitaemia detected on a Giemsa-stained thick smear (Greenwood and Armstrong, 1991). CM was defined according to the WHO criteria: a coma score < 3 on the Blantyre Scale for children < 60 months, or a coma score < 7 on the Glasgow Scale for children ≥ 60 months. Meningitis and encephalitis were ruled out by cerebrospinal fluid analysis after lumbar puncture. Exclusion criteria were different known aetiologies of encephalopathy and hypoglycaemia (glycaemia < 40 mg/dl). Patients with consciousness disturbances or with other diseases were also excluded from this group. The UM group represents patients with malaria diagnosis and febrile illness without any clinical finding suggestive of other causes of infection and with no manifestations of severe malaria. Enrollment of UIF controls excluded children with any clinical finding suggestive of illness and the UIF status was confirmed by the absence of Plasmodium DNA in the peripheral blood as detected by PCR (Snounou, 1996).

Genotyping

Genomic DNA was extracted from whole blood using the Chemagen Magnetic Bead technology. DNA preparations were quantified using PicoGreen reagents according to the supplier instructions. 27 SNPs covering the *IFNAR1* region were initially genotyped using the Sequenom's iPlex assay (San Diego, USA) and the Sequenom MassArray K2 platform performed by the Genomics Unit of the Instituto Gulbenkian de Ciência.

Extensive quality control was performed using eight HapMap (http://hapmap.ncbi.nlm.nih.gov/) controls of diverse ethnicity, Hardy-Weinberg equilibrium (HWE) with $P > 0.01$ in controls and $P > 0.0001$ in cases, and a minimum of 90% call rate for each SNP. Genotype determinations were performed blinded to affection status. Only SNPs with minor allele frequency > 1% in both case and controls groups were analyzed for association. Nine SNPs in *IFNAR1* (rs224359, rs2252930, rs12626750, rs2834197, rs2226300, rs2254315, rs1012943, 2843996 and 2254305) did not meet the quality control criteria and were excluded. Samples with < 75% call rate and duplicates were excluded from analysis, a total of 47 samples were excluded. The final dataset used in the analysis consisted of 544 subjects comprising 110 CM patients, 129 UM patients and 305 UIF controls (Table S1).

Association testing

$\chi 2$ tests for HWE in controls and in cases, allelic and haplotypic association of SNPs with malaria and cerebral malaria risk, and progression to CM, and linkage disequilibrium (LD) plots were performed using Haploview 4.2 (Barrett et al., 2005). Diagram with representation of allelic genetic association results was produced by the snp.plotter R package (Luna and Nicodemus, 2007). Association analyses were performed with logistic regression using the SNPassoc v.1.4-9 package (Gonzalez et al., 2007) implemented in the R freeware (http://cran.r-project.org/). Results were considered suggestive below the conventional probability level of 0.05. Bonferroni corrections for multiple tests were carried out to exclude type I errors (the significance level for 18 tests is set at P value < 2.78 E−3).

Animals

Male, 8-12 weeks old C57BL/6, B6.Ly5.1, *Ifnar1-/-* and BALB/c mice were bred and used as provided by the Instituto Gulbenkian de Ciência in-house animal facility. *Ifnar1-/-* mice were originally a gift to the institute from Michel Aquet (*Ifnar1*$^{\text{-tm-Agt}}$) (Muller et al., 1994). *Ifnar1-/-* mice have been backcrossed into the C57BL/6 background, (98.7% - 99.36% C57BL/6 background outside of the congenic region, as confirmed by the animal facility at Instituto Gulbenkian de Ciência). All procedures were in accordance with national regulations on animal experimentation and welfare as approved by the Instituto Gulbenkian de Ciência Ethics committee.

Parasite, infection and ECM disease assessment

All infections used 1×10^6 *P.berghei ANKA*-GFP parasitized iRBC (Franke-Fayard et al., 2004) given via i.p injection. Frozen iRBC stocks were expanded in C57BL/6 mice prior to infection. Parasitemia was determined as the % of GFP+ red blood cells, using flow cytometry analysis (FacScan Cell Analyser, Becton Dickinson, New Jersey) and non-infected RBCs as negative control. ECM development was monitored from day 5 post-infection (PI) as including; head deviations, paralysis, ataxia and convulsions (Pamplona et al., 2007). ECM susceptible mice developed symptoms at days 6-7 PI and died within 4-5 hours. Mice resistant to ECM died around days 22-25 from anemia and hyperparasitemia without displaying neurological symptoms.

Blood brain barrier (BBB) integrity.

Upon display of ECM induced coma in C57BL/6 mice, the experimental groups of mice were successively injected with 100 μl of 2% Evan's blue dye (Sigma), sacrificed one hour post injection and perfused intracardially with 15 ml ice-cold PBS. Brains were dissected, weighed and immersed in 2 ml formamide (Merck) covered at 37 °C for 48 h, to allow extraction of Evan's blue dye, images were taken after the 48 h period. Non-infected mice from each group were used as controls. Absorbance of dye was measured at wavelengths 620 nm and 740 nm using Spectrophotometry, (ThermoSpectronic, Helios Delta). Using a standard curve, data was calculated and expressed as μg of Evans blue dye/mg of brain tissue.

Histology

Infected C57BL/6 and *Ifnar1-/-* mice were sacrificed upon observation of clinical signs of ECM in C57BL/6 mice, around day 6 PI. Non-infected C57BL/6 and *Ifnar1-/-* mice were used as controls and sacrificed at the same time point. For hematoxylin and eosin (H&E) staining; brains were carefully removed, fixed in 10% neutral-buffered formalin, embedded, sectioned (4 μm) and mounted with entellan (Merck, Darmstadt, Germany) then finally stained with Hematoxylin and Eosin following standard procedures. CM and brain pathology were assessed by routine histopathology in coronal brain sections of the same anatomical location. Bright field images were captured utilizing a Leica DMD108 microscope (LeicaMicrosystems), 10 × (numerical aperture: 0.40) and 40 × (numerical aperture: 0.95) objectives were employed. Adobe Photoshop software was utilized to compose images and adjust the contrast (Adobe, USA).

Gene expression

C57BL/6 and *Ifnar1-/-* infected mice were sacrificed at days 5, 6, and 7 PI. *Ifnar1-/-* mice were sacrificed further at days 9 and 11 PI, C57BL/6 mice were not collected at these time points due to death from ECM. Non-infected C57BL/6 and *Ifnar1-/-* mice were used as controls and displayed as day 0. Brains were dissected, fast frozen in liquid nitrogen and stored at -80 °C. Brains were then homogenized and a final brain weight of 20 mg was used for total RNA extraction (RNeasy® Mini Kit, Qiagen). RNA quality was determined using Nanodrop and a final elution of 50 μl extracted. One microgram of total RNA was converted to cDNA (Transcriptor High Fidelity cDNA Synthesis Kit, Roche) using random hexamer primers and a final volume of 10 μl of the cDNA reaction was diluted 1:3 in RNAse-free water to be used for mRNA quantification. *Tnf-α*, *Il-10* mRNA was quantified using TaqMan® Gene Expression Assays from ABI (Mm00443258_m1 and Mm99999062_m1, respectively). *Plasmodium berghei ANKA* rRNA was quantified using specific primer sequences: Forward 5'-CCG ATA ACG AAC GAG ATC TTA ACC T-3', Reverse 5'-CGT CAA AAC CAA TCT CCC AAT AAA GG-3' and Probe 5'-ACT CGC CGC TAA TTA G-3' (FAM/MGB), all with Taqman® Universal PCR Master Mix. T lymphocyte (*Cd3e)* expression was quantified using specific primer sequence: Forward 5'-TCT CGG AAG TCG AGG ACA GT-3' Reverse 5'-ATC AGC AAG CCC AGA GTG AT-3' (Epiphanio et al., 2008), using Power SYBR Green PCR Master Mix (Applied Biosystems). Gene expression quantification reactions were performed on an ABI Prism 7900HT system according to manufacturers' instructions, a total volume of 10 μl PCR reactions was amplified for 45 cycles. Relative quantification of specific mRNA was normalized to the mouse housekeeping gene *ACTB* (Mouse ACTB Endogenous Controls, ABI), used in multiplex PCR with the target genes and calculated using the ΔΔCt method.

Pre-Sensitization protocol

For infected blood donor mice; blood was collected by mandibular vein puncture into an eppendorf containing 10 μl of Heparin (Heparina Leo, Leo Pharmaceutical products) from infected mouse at day 6 PI, upon display of ECM symptoms and when parasitemia was around 30%. Parasitemia was measured to calculate injection of 4×10^6 iRBC into cell donor mice. Collected blood was then placed on ice in a 50 ml falcon tube and irradiated at 20 k Rad (GAMMACELL 2000, MØLSGAARD Medical Denmark). Irradiated iRBC were then re-suspended in PBS and injected i.p into cell donor mice. At day 6 post irradiated-iRBC injection, cell donor mice were sacrificed and spleens processed for cell transfer. For non-infected blood donor mice used as controls; mice were bled and an equivalent volume of non-infected RBC were irradiated and diluted in PBS in the same manner as above.

Spleen cell transfers

Single cell suspensions were prepared from spleens of cell donor mice. For total spleen cell transfers; cells were washed 2 × in PBS, counted in a hemocytometer, re-suspended in PBS and injected 5×10^6/ 100 μl into recipient mice. For spleen $CD8^+$ cell transfers; cells were washed 2 × in PBS 2%FCS and incubated with anti-mouse CD8-alexa647 antibody (clone YTS169, in house production), for 30 min on ice. For $CD8^+$Ly5.1/2+ cell transfers; cells were incubated with anti-mouse CD8-alexa647 antibody (clone YTS169, in house production), anti-mouse CD45.1-FITC antibody (clone 820, BD Pharmingen) or anti-mouse CD45.2-PE antibody (clone 104.2, in house production) for 30 min on ice. Stained cells were washed in PBS 2%FCS and sorted (FacsAria Multicolour Cell Sorter, Becton Dickinson, New Jersey) by combining lymphocyte morphological gating and relevant antibody labels. For $CD8^+$ transfers; cells were collected as purified $CD8^+$ cells and CD8- (depleted) groups of cells. For CD8+Ly5.1/2 transfers; cells were gated for $CD8^+$ cells within which CD45.1+ or CD45.2+ populations were collected. Purified cell populations were washed in PBS and counted. Cells were injected intravenously (i.v) 3×10^6/ 100 μl into recipient mice. Respective groups of recipient mice were then infected 1×10^6 iRBC/ 100 μl *PbA* one hour after cell transfer. Mice were monitored for parasitemia and ECM development from day 5 PI.

Analysis of spleen cells

Single cell suspensions were prepared from spleens of C57BL/6 and *Ifnar1-/-* infected mice at day 5 PI, non-infected mice from both groups were used as control. Cells were then washed and re-suspended in red blood cell lysis, then washed and re-suspended in 100 μl RPMI medium supplemented with 10% FCS, 10 U/ml Pen-Strep, 1% sodium pyruvate, 1% HEPES 1M, 1% L-Glutamine, 0.01% β-Mercaptoethanol, centrifuged and finally re-suspended in 200 μl RPMI supplemented medium containing 10 μg/ml of Brefeldin A for fixation of cytokine production, 100 ng/ml of PMA and 500 ng/ml of Ionomycin for cell stimulation. Cells were stimulated at 37 °C, 5% CO_2 for 4 hours. Cells were then processed for extracellular staining; cells were centrifuged, pelleted and re-suspended in Fc Block for 20 min on ice, cells were then washed in PBS, 2%FCS, and re-suspended in anti-mouse CD8-alexa647 antibody (clone YTS169, in house antibody) for 20 min on ice. Cells were then washed and re-suspended in 2%PFA for fixation for 30min at room temperature (RT), then washed 2 × in PBS and re-suspended in 200 μl PBS, 2%FCS and stored at 4 °C overnight. The proceeding day, cells were pelleted, re-suspended in permeabilisation buffer (10% Saponin in PBS, 2%FCS) for 10 min at RT in preparation for intracellular staining. Cells were then washed and pelleted and incubated with anti-mouse GranzymeB-FITC (clone NGZB, eBioscience) and anti mouse IFN-γ-PE (clone XMG1.2, BD Pharmingen) for 30 min at RT. Cells were then washed 2 × in permeabilisation buffer and then 2 × in PBS, 2%FCS and re-suspended in 150 μl PBS, 2%FCS plus 5×10^5 beads (Beckman Coulter ® nominal 10μm Latex Beads). Cell analysis was performed using FacsCalibur cell analyzer, and FlowJo (version 7) for analysis. Single staining preparations were used for control compensation of double staining analysis.

Analysis of brain-sequestered leukocytes

C57BL/6 and *Ifnar1-/-* infected mice were sacrificed at day 6 PI, perfused pericardially (as described above) and brains placed in 10 ml of HBSS supplemented with Collagenase VIII (Sigma-Aldrich), 0.2 mg/ml. Brains were then smashed and incubated for 30 min at 37 °C. Each sample was passed through a 100 μm strainer and centrifuged for 10 min at 1500 rpm. Supernatant was discarded and samples re-suspended in 10 ml PBS and centrifuged. Samples were re-suspended in 10 ml of 30% Percoll gradient (Percoll™, GE Healthcare, BioSciences) and centrifuged for 20 min at 2500 rpm at RT, without brake. The supernatant was carefully aspirated and pellet re-suspended in 50 ml of PBS and centrifuged. The supernatant was discarded and each sample pellet re-suspended to a final volume of 200 μl. Cells were centrifuged and re-suspended in 100 μl red blood cell lysis, incubated for 5 min at RT, washed 2 × in 200 μl PBS, 2%FCS and re-suspended in supplemented RPMI medium and proceeded for extra and intracellular staining and analysis as described above.

Statistical Analysis

Student's unpaired, two-tailed *t*-test was used for analysis in cases of two comparative groups of mouse data. One-way ANOVA was used in comparing three or more groups of data. Survival analysis was assessed by Log rank Test; all performed using Prism GraphPad 4. $P \leq 0.05$ was considered statistically significant.

Online Supplemented Material

We include as supplemental material, Fig. S1 showing control groups for non-infected cell transfer experiments and Fig. S2 showing mean fluorescence intensity (MFI) data for brain sequestered leucocytes. Table S1 details the human sample collection analyzed in this study, Table S2 shows the results of the allelic association tests and Table S3 shows the results of the genotypic association tests reported in this paper.

Acknowledgments

We are most grateful to the children that participated in this study and thank the staff of the Hospital Pediátrico David Bernardino, Drs. Filomena Silva, Emingarda Castelo Branco and Rosa Silva from the Instituto de Saúde Pública de Angola for the help on sample processing and Dr. Rui from the Clínica Sagrada Esperança de Luanda for sample collection materials. We thank Miguel Soares, (Instituto Gulbenkian de Ciência) for access to reagents and scientific discussion and thank Ivo Marguti for technical support and discussion. We thank Dr. Tânia Carvalho, resident pathologist at Instituto Gulbenkian de Ciência for analysis of pathology samples and Rui Gardner and Telma Lopes for expertise in cell sorting.

This work is supported by Fundação para a Ciência e a Technologia fellowship grant: SFRH / BD / 33564 / 2008.

The authors have no conflicting financial interests.

Author contributions E. Ball performed mouse experiments and data analysis. M. R. Sambo, C. Benchimol orchestrated human sample collections. M. R. Sambo, M. J. Trovoada, L. A. Gonçalves, J. Sobral performed sample processing and genotyping. M. R. Sambo, M. Martins conducted the genetic analysis. E. Ball, M. Martins and C. P. Gonçalves wrote the paper. A. Coutinho and C. P. Gonçalves conceived the study. All authors discussed the results and commented at critical points of the manuscript preparations.

References

Aucan, C., A.J. Walley, B.J. Hennig, J. Fitness, A. Frodsham, L. Zhang, D. Kwiatkowski, and A.V. Hill. 2003. Interferon-alpha receptor-1 (IFNAR1) variants are associated with protection against cerebral malaria in the Gambia. *Genes Immun* 4:275-282.

Barrett, J.C., B. Fry, J. Maller, and M.J. Daly. 2005. Haploview: analysis and visualization of LD and haplotype maps. *Bioinformatics* 21:263-265.

Belnoue, E., M. Kayibanda, A.M. Vigario, J.C. Deschemin, N. van Rooijen, M. Viguier, G. Snounou, and L. Renia. 2002. On the pathogenic role of brain-sequestered alphabeta CD8+ T cells in experimental cerebral malaria. *J Immunol* 169:6369-6375.

Carvalho, L.J. 2010. Murine cerebral malaria: how far from human cerebral malaria? *Trends Parasitol* 26:271-272.

Combes, V., F. El-Assaad, D. Faille, R. Jambou, N.H. Hunt, and G.E. Grau. 2010. Microvesiculation and cell interactions at the brain-endothelial interface in cerebral malaria pathogenesis. *Prog Neurobiol* 91:140-151.

Craig, A.G., G.E. Grau, C. Janse, J.W. Kazura, D. Milner, J.W. Barnwell, G. Turner, and J. Langhorne. 2012. The role of animal models for research on severe malaria. *PLoS Pathog* 8:e1002401.

de Souza, J.B., J.C. Hafalla, E.M. Riley, and K.N. Couper. 2010. Cerebral malaria: why experimental murine models are required to understand the pathogenesis of disease. *Parasitology* 137:755-772.

deWalick, S., F.H. Amante, K.A. McSweeney, L.M. Randall, A.C. Stanley, A. Haque, R.D. Kuns, K.P. MacDonald, G.R. Hill, and C.R. Engwerda. 2007. Cutting edge: conventional dendritic cells are the critical APC required for the induction of experimental cerebral malaria. *J Immunol* 178:6033-6037.

Diop, G., T. Hirtzig, H. Do, C. Coulonges, A. Vasilescu, T. Labib, J.L. Spadoni, A. Therwath, M. Lathrop, F. Matsuda, and J.F. Zagury. 2006. Exhaustive genotyping of the interferon alpha receptor 1 (IFNAR1) gene and association of an IFNAR1 protein variant with AIDS progression or susceptibility to HIV-1 infection in a French AIDS cohort. *Biomed Pharmacother* 60:569-577.

Driss, A., J.M. Hibbert, N.O. Wilson, S.A. Iqbal, T.V. Adamkiewicz, and J.K. Stiles. 2011. Genetic polymorphisms linked to susceptibility to malaria. *Malar J* 10:271.

e Pinto, E.A., and J.G. Alves. 2008. The causes of death of hospitalized children in Angola. *Trop Doct* 38:66-67.

Epiphanio, S., S.A. Mikolajczak, L.A. Goncalves, A. Pamplona, S. Portugal, S. Albuquerque, M. Goldberg, S. Rebelo, D.G. Anderson, A. Akinc, H.P. Vornlocher, S.H. Kappe, M.P. Soares, and M.M. Mota. 2008. Heme oxygenase-1 is an anti-inflammatory host factor that promotes murine plasmodium liver infection. *Cell Host Microbe* 3:331-338.

Ferreira, A., I. Marguti, I. Bechmann, V. Jeney, A. Chora, N.R. Palha, S. Rebelo, A. Henri, Y. Beuzard, and M.P. Soares. 2011. Sickle hemoglobin confers tolerance to Plasmodium infection. *Cell* 145:398-409.

Franke-Fayard, B., H. Trueman, J. Ramesar, J. Mendoza, M. van der Keur, R. van der Linden, R.E. Sinden, A.P. Waters, and C.J. Janse. 2004. A Plasmodium

berghei reference line that constitutively expresses GFP at a high level throughout the complete life cycle. *Mol Biochem Parasitol* 137:23-33.
Galea, I., M. Bernardes-Silva, P.A. Forse, N. van Rooijen, R.S. Liblau, and V.H. Perry. 2007. An antigen-specific pathway for CD8 T cells across the blood-brain barrier. *J Exp Med* 204:2023-2030.
Gonzalez, J.R., L. Armengol, X. Sole, E. Guino, J.M. Mercader, X. Estivill, and V. Moreno. 2007. SNPassoc: an R package to perform whole genome association studies. *Bioinformatics* 23:644-645.
Greenwood, B.M., and J.R. Armstrong. 1991. Comparison of two simple methods for determining malaria parasite density. *Trans R Soc Trop Med Hyg* 85:186-188.
Haque, A., S.E. Best, A. Ammerdorffer, L. Desbarrieres, M.M. de Oca, F.H. Amante, F. de Labastida Rivera, P. Hertzog, G.M. Boyle, G.R. Hill, and C.R. Engwerda. 2011a. Type I interferons suppress CD4 T-cell-dependent parasite control during blood-stage Plasmodium infection. *Eur J Immunol* 41:2688-2698.
Haque, A., S.E. Best, K. Unosson, F.H. Amante, F. de Labastida, N.M. Anstey, G. Karupiah, M.J. Smyth, W.R. Heath, and C.R. Engwerda. 2011b. Granzyme B expression by CD8+ T cells is required for the development of experimental cerebral malaria. *J Immunol* 186:6148-6156.
Hermsen, C., T. van de Wiel, E. Mommers, R. Sauerwein, and W. Eling. 1997. Depletion of CD4+ or CD8+ T-cells prevents Plasmodium berghei induced cerebral malaria in end-stage disease. *Parasitology* 114 (Pt 1):7-12.
Hervas-Stubbs, S., J.L. Perez-Gracia, A. Rouzaut, M.F. Sanmamed, A. Le Bon, and I. Melero. 2011. Direct effects of type I interferons on cells of the immune system. *Clin Cancer Res* 17:2619-2627.
Huys, L., F. Van Hauwermeiren, L. Dejager, E. Dejonckheere, S. Lienenklaus, S. Weiss, G. Leclercq, and C. Libert. 2009. Type I interferon drives tumor necrosis factor-induced lethal shock. *J Exp Med* 206:1873-1882.
Issifou, S., E. Kendjo, M.A. Missinou, P.B. Matsiegui, A. Dzeing-Ella, F.A. Dissanami, M. Kombila, S. Krishna, and P.G. Kremsner. 2007. Differences in presentation of severe malaria in urban and rural Gabon. *Am J Trop Med Hyg* 77:1015-1019.
Ito, T., H. Kanzler, O. Duramad, W. Cao, and Y.J. Liu. 2006. Specialization, kinetics, and repertoire of type 1 interferon responses by human plasmacytoid predendritic cells. *Blood* 107:2423-2431.
Khor, C.C., F.O. Vannberg, S.J. Chapman, A. Walley, C. Aucan, H. Loke, N.J. White, T. Peto, L.K. Khor, D. Kwiatkowski, N. Day, A. Scott, J.A. Berkley, K. Marsh, N. Peshu, K. Maitland, T.N. Williams, and A.V. Hill. 2007. Positive replication and linkage disequilibrium mapping of the chromosome 21q22.1 malaria susceptibility locus. *Genes Immun* 8:570-576.
Kolumam, G.A., S. Thomas, L.J. Thompson, J. Sprent, and K. Murali-Krishna. 2005. Type I interferons act directly on CD8 T cells to allow clonal expansion and memory formation in response to viral infection. *J Exp Med* 202:637-650.
Le Bon, A., V. Durand, E. Kamphuis, C. Thompson, S. Bulfone-Paus, C. Rossmann, U. Kalinke, and D.F. Tough. 2006. Direct stimulation of T cells by type I IFN enhances the CD8+ T cell response during cross-priming. *J Immunol* 176:4682-4689.

Luna, A., and K.K. Nicodemus. 2007. snp.plotter: an R-based SNP/haplotype association and linkage disequilibrium plotting package. *Bioinformatics* 23:774-776.
Lundie, R.J., T.F. de Koning-Ward, G.M. Davey, C.Q. Nie, D.S. Hansen, L.S. Lau, J.D. Mintern, G.T. Belz, L. Schofield, F.R. Carbone, J.A. Villadangos, B.S. Crabb, and W.R. Heath. 2008. Blood-stage Plasmodium infection induces CD8+ T lymphocytes to parasite-expressed antigens, largely regulated by CD8alpha+ dendritic cells. *Proc Natl Acad Sci U S A* 105:14509-14514.
Mackintosh, C.L., J.G. Beeson, and K. Marsh. 2004. Clinical features and pathogenesis of severe malaria. *Trends Parasitol* 20:597-603.
Marrack, P., J. Kappler, and T. Mitchell. 1999. Type I interferons keep activated T cells alive. *J Exp Med* 189:521-530.
Milner, D.A., Jr. 2010. Rethinking cerebral malaria pathology. *Curr Opin Infect Dis* 23:456-463.
Miu, J., N.H. Hunt, and H.J. Ball. 2008. Predominance of interferon-related responses in the brain during murine malaria, as identified by microarray analysis. *Infect Immun* 76:1812-1824.
Muller, U., U. Steinhoff, L.F. Reis, S. Hemmi, J. Pavlovic, R.M. Zinkernagel, and M. Aguet. 1994. Functional role of type I and type II interferons in antiviral defense. *Science* 264:1918-1921.
Newton, C.R., and S. Krishna. 1998. Severe falciparum malaria in children: current understanding of pathophysiology and supportive treatment. *Pharmacol Ther* 79:1-53.
Nitcheu, J., O. Bonduelle, C. Combadiere, M. Tefit, D. Seilhean, D. Mazier, and B. Combadiere. 2003. Perforin-dependent brain-infiltrating cytotoxic CD8+ T lymphocytes mediate experimental cerebral malaria pathogenesis. *J Immunol* 170:2221-2228.
Pamplona, A., A. Ferreira, J. Balla, V. Jeney, G. Balla, S. Epiphanio, A. Chora, C.D. Rodrigues, I.P. Gregoire, M. Cunha-Rodrigues, S. Portugal, M.P. Soares, and M.M. Mota. 2007. Heme oxygenase-1 and carbon monoxide suppress the pathogenesis of experimental cerebral malaria. *Nat Med* 13:703-710.
Prinz, M., H. Schmidt, A. Mildner, K.P. Knobeloch, U.K. Hanisch, J. Raasch, D. Merkler, C. Detje, I. Gutcher, J. Mages, R. Lang, R. Martin, R. Gold, B. Becher, W. Bruck, and U. Kalinke. 2008. Distinct and nonredundant in vivo functions of IFNAR on myeloid cells limit autoimmunity in the central nervous system. *Immunity* 28:675-686.
Razakandrainibe, R., S. Pelleau, G.E. Grau, and R. Jambou. 2012. Antigen presentation by endothelial cells: what role in the pathophysiology of malaria? *Trends Parasitol* 28:151-160.
Renia, L., A.C. Gruner, and G. Snounou. 2010. Cerebral malaria: in praise of epistemes. *Trends Parasitol* 26:275-277.
Riley, E.M., K.N. Couper, H. Helmby, J.C. Hafalla, J.B. de Souza, J. Langhorne, W.B. Jarra, and F. Zavala. 2010. Neuropathogenesis of human and murine malaria. *Trends Parasitol* 26:277-278.
Sambo, M.R., M.J. Trovoada, C. Benchimol, V. Quinhentos, L. Goncalves, R. Velosa, M.I. Marques, N. Sepulveda, T.G. Clark, S. Mustafa, O. Wagner, A. Coutinho, and C. Penha-Goncalves. 2010. Transforming growth factor beta 2 and heme oxygenase 1 genes are risk factors for the cerebral malaria syndrome in Angolan children. *PLoS One* 5:e11141.

Sharma, S., R.B. DeOliveira, P. Kalantari, P. Parroche, N. Goutagny, Z. Jiang, J. Chan, D.C. Bartholomeu, F. Lauw, J.P. Hall, G.N. Barber, R.T. Gazzinelli, K.A. Fitzgerald, and D.T. Golenbock. 2011. Innate immune recognition of an AT-rich stem-loop DNA motif in the Plasmodium falciparum genome. *Immunity* 35:194-207.

Snounou, G. 1996. Detection and identification of the four malaria parasite species infecting humans by PCR amplification. *Methods Mol Biol* 50:263-291.

Song le, H., N.T. Xuan, N.L. Toan, V.Q. Binh, A.B. Boldt, P.G. Kremsner, and J.F. Kun. 2008. Association of two variants of the interferon-alpha receptor-1 gene with the presentation of hepatitis B virus infection. *Eur Cytokine Netw* 19:204-210.

Stewart, T.A. 2003. Neutralizing interferon alpha as a therapeutic approach to autoimmune diseases. *Cytokine Growth Factor Rev* 14:139-154.

Figure Legends

Figure 1. IFNAR1 gene SNP alleles protect against malaria progression to cerebral malaria syndrome but confer increased susceptibility to malaria infection. Results of genetic association tests for minor frequency alleles at 18 *IFNAR1* SNPs, depicted at the bottom of the horizontal axis according to relative physical distance. Black symbols represent results of malaria susceptibility tests obtained by comparing 129 patients with uncomplicated malaria (UM) and 305 uninfected controls (UIF) and gray symbols represent tests of susceptibility against progression to cerebral malaria (CM) obtained by comparing 110 cases of CM and 129 UM patients. (a) Scaled diagram of the *IFNAR1* gene structure: exons are represented by black boxes and marked with its corresponding number; 5'UTR and 3'UTR are represented by gray boxes; introns are represented by black lines between exons. (b) Individual alleles *P*-value of association tests using χ^2 tests. Thresholds for suggestive association ($P = 0.05$) and for significant association after multiple testing Bonferroni correction ($P = 2.78$ E−3) are represented. (c) Genetic effects of minor frequency alleles at the 18 indicated *IFNAR1* SNPs, as ascertained by the Odds Ratio. (d) Linkage Disequilibrium plot representing pairwise R-square in a gray scale and revealing the two haplotype blocks in the analyzed region. This diagram is an adaptation of the figure produced by the snp.plotter R package and the LD map obtained from Haploview 4.2.

Figure 2. *Ifnar1-/-* mice are protected from ECM and show no decrease in parasite burden. C57BL/6 (filled squares) and *Ifnar1-/-* (open circles) mice were infected with 1×10^6 *P.berghei* ANKA-GFP (*PbA*) infected red blood cells (iRBC) via intraperitoneal (i.p) injection. (a) Survival curve ($n = 17$, log-rank rest;

***$P \leq 0.001$). (b) Parasitemia progression ($n = 17$, unpaired, two tailed *t*-test; day 6 post-infection (PI); **$P = 0.0016$, day 7 PI; **$P = 0.0021$). Data collective from at least four independent experiments. Time window of C57BL/6 ECM development is shadowed.

Figure 3. *Ifnar1-/-* mice are protected from BBB breakage and show reduced mononuclear cell accumulation in brain microvasculature. C57BL/6, *Ifnar1-/-* and BALB/c mice were infected with 1×10^6 *PbA* iRBC i.p. (a) At day 6 PI, BBB integrity was assessed in all infected groups of mice by Evan's Blue perfusion. Non-infected mice from each group were used as controls. (n = 3-5 mice per group). Images representative of two independent experiments. (b) Quantification of Evan's Blue dye was measured as μg of dye/mg of brain tissue, (n = 3-4 mice per group, ANOVA, Tukey's Multiple Comparison Test; ***$P \leq 0.001$). Data representative of two independent experiments. (c-j) H&E staining of brain sections from C57BL/6 and *Ifnar1-/-* mice on day 6 PI, infected 1×10^6 *PbA*, and non-infected mice as controls. Mice were sacrificed upon display of ECM in C57BL/6 mice. Coronal sections of brain microvasculature and mononuclear cell accumulation in; non-infected C57BL/6 mouse (c), infected C57BL/6 mouse (d-f), non-infected *Ifnar1-/-* mouse (g), infected *Ifnar1-/-* mouse (h-j); magnification × 400, bar 30 μm. Coronal sections of infected C57BL/6 mice blood vessel, showing absence of endothelial cells (e, arrows) and presence of hemorrhagic foci with iRBCs (f, arrowhead). Sections of infected *Ifnar1-/-* mice blood vessel, showing intact endothelial cells (j, arrow), and intra-luminal iRBCs (i and j, arrowhead); magnification × 1000, bar 30 μm. Images represent one of three mice examined per group.

Figure 4. Parasite accumulation and brain inflammation markers in *Ifnar1-/-* infected mice. C57BL/6 and *Ifnar1-/-* mice were infected 1×10^6 *PbA* iRBC, i.p. and brain RNA extracted at indicated days for RT-PCR quantification after normalisation to endogenous control *ACTB*. (a) *P.berghei* rRNA relative quantification, day 5 infected C57BL/6 mice is used as calibrator. Gene expression of *Cd3* (b), *Tnf-α* (c) and *Il-10* (d) quantification, non-infected C57BL/6 mice is used as a calibrator; represented as day 0. (n = 3-4 mice per group/per day, unpaired, two tailed *t*-test; *$P \leq 0.05$, **$P \leq 0.01$). Data presented as means ± SD from two independent experiments. Time window of C57BL/6 ECM onset is shadowed.

Figure 5. *Ifnar1-/-* mice succumb to ECM upon cell transfer of parasite-sensitized splenocytes, explicitly $CD8^+$ cells. (a) Schematic representation of pre-sensitization protocol: Blood donor mice were infected 1×10^6 *PbA* i.p, at day 6 PI mice were bled and iRBCs irradiated and injected into cell donor mice (represents Day 0 on schematic). Day 6 post-irradiation iRBC injection, cell donor mice were sacrificed and spleen cell suspensions were stained and purified by sorting. Purified cell populations were injected back into selected groups of recipient mice that were either left non-infected or infected one hour after cell transfer with 1×10^6 *PbA* i.p. Recipient mice were then monitored from day 5 PI for parasitemia levels in peripheral blood and ECM development. Non-infected blood donor mice were used as controls, non-infected RBC were irradiated and injected in the same manner as infected. (b-e) Parasitemia and survival curves of *Ifnar1-/-* mice recipients of spleen cells, (n = 4-6 mice were used per group in each experiment). (b) *Ifnar1-/-* recipient mice that received total spleen cells (Spl) from C57BL/6 non-exposed cell donor mice (open squares) and control infected *Ifnar1-/-* mice that received no cell transfer (open

diamonds). (c) *Ifnar1-/-* recipient mice that received total spleen cells from C57BL/6 pre-exposed cell donor mice that had received irradiated iRBC (see fig.5) and were subsequently infected (open squares) or were left non-infected (closed squares). (d) *Ifnar1-/-* recipient mice that received sorted pre-sensitized $CD8^+$ spleen cells (open squares) or sorted pre-sensitized CD8-depleted spleen cells (open circles) from C57BL/6 pre-exposed cell donor mice that had received irradiated iRBC; transfer control is represented by infected *Ifnar1-/-* mice that received no cell transfer (diamonds). (e) *Ifnar1-/-* mice that received sorted pre-sensitized $CD8^+$ spleen cells (open squares) or sorted pre-sensitized CD8-depleted spleen cells (open circles) from *Ifnar1-/-* pre-exposed cell donor mice that had received irradiated iRBC. (n = 4-6 mice per group, parasitemia; unpaired, two tailed t-test, survival curves; Log-rank Test). Each plot represents one of at least two independent experiments performed. Time window of cerebral malaria manifestations is shadowed in survival plots. (f) Measurement of BBB breakage by Evans Blue dye perfusion in *Ifnar1-/-* mice that received cell transfers as in (d) and were sacrificed on day 6 PI upon display of ECM by mice that received $CD8^+$ cells and infection, (n = 3-4 per group). (g) Quantification of Evan's Blue dye measured as μg of dye/mg of brain tissue, (n = 3-4 per group, ANOVA, Tukey's Multiple Comparison Test; $^{**}P \leq 0.01$, $^{***}P \leq 0.001$). Data (f and g) represent one of two independent experiments.

Figure 6. Intrinsic *Ifnar1-/-* $CD8^+$ cell impairment protects from ECM.

(a) Schematic representation of experimental protocol: Non-infected *Ifnar1-/-* mice were used as donors of 5×10^6 $CD8^+$Ly5.2+ cells that were transferred to previously non-lethally irradiated B6.Ly5.1 recipient mice. 6 days post transfer Ly5.1/Ly5.2 chimeric mice received 4×10^6 irradiated iRBC from a previously infected B6.Ly5.1

mouse. (b) 7 days after iRBC infection $CD8^+$Ly5.2+ and $CD8^+$Ly5.1+ spleen cells from chimeric mice were FACS-sorted as described in the material and methods. Sorted $CD8^+$ cells were injected back into recipient groups of *Ifnar1-/-* mice. Recipient mouse were then infected 1×10^6 iRBC one hour after cell transfer. (c) Parasitemia and survival curves of *Ifnar1-/-* recipient mice that received either $CD8^+$Ly5.1+ or $CD8^+$Ly5.2+ cells (as described in a). Control *Ifnar1-/-* mice were used that received no cell transfer and infection only. (n = 3-12 mice per group, parasitemia; unpaired, two tailed t-test between $CD8^+$Ly5.1+ and $CD8^+$Ly5.2+ recipient groups; $*P \leq 0.05$, survival curves; Log-rank Test). Data pooled from three independent experiments. Time window of C57BL/6 ECM manifestations is shadowed in survival plot.

Figure 7. *Ifnar1-/-* $CD8^+$ T cells display activation phenotype upon *P.berghei* infection but do not accumulate in the brain.

Number of $CD8^+$ T cells, GrB+ $CD8^+$ T cells, and IFN-γ+ $CD8^+$ T cells in the spleen (a-c), (C57BL/6 non-infected group mean; 2.8×10^5, *Ifnar1-/-* non-infected group mean; 8.0×10^4) and in perfused brains (d-f) of infected and non-infected C57BL/6 and *Ifnar1-/-* mice, and in perfused brains of *Ifnar1-/-* recipient mice (g-i) that received pre-sensitized sorted $CD8^+$ or CD8-depleted spleen cells from C57BL/6 pre-sensitized cell donor mice that had received irradiated iRBC (as in Fig. 5). Mice infected 1×10^6 *PbA* were analysed for $CD8^+$ T cells in the spleen on day 5 PI and in the brain on day 6 PI when C57BL/6 or *Ifnar1-/-* ECM induced-mice displayed symptoms of ECM development. (n = 3-5 mice per group, unpaired, two tailed t-test; $*P \leq 0.05$, $**P \leq 0.01$, $***P \leq 0.001$). Data is representative of three (a-f) or two (g-i) independent experiments performed.

Supplemental Figure Legends

Fig. S1. Transfer of non-exposed $CD8^+$ C57BL/6 cells cannot induce ECM in *Ifnar1-/-* mice. (a) *Ifnar1-/-* recipient mice that received sorted $CD8^+$ spleen cells (open squares) or sorted CD8-depleted spleen cells (open circles) from C57BL/6 non-exposed cell donor mice that had received irradiated non-infected RBC; transfer control is represented by infected *Ifnar1-/-* mice that received no cell transfer (diamonds). (b) *Ifnar1-/-* mice that received sorted $CD8^+$ spleen cells (open squares) or sorted CD8-depleted spleen cells (open circles) from *Ifnar1-/-* cell donor mice that had received irradiated non-infected RBC. (*n* = 3-6 mice per group, parasitemia; unpaired, two tailed *t*-test performed between $CD8^+$ and CD8-depleted cell transfer recipient groups; *$P \leq 0.05$, **$P \leq 0.01$, survival curves; Log-rank Test). Each plot represents one of at least two independent experiments performed. Time window of C57BL/6 ECM manifestations is shadowed in survival plots.

Fig. S2. *Ifnar1-/-* $CD8^+$ T cells show cytotoxic ability like that of C57BL/6 mice. Mean fluorescence intensity (MFI) of GrB+ on $CD8^+$ T cells (a) and IFN-γ+ on $CD8^+$ T cells (b) in perfused brains of infected and non-infected C57BL/6 and *Ifnar1-/-* mice, infected 1×10^6 *PbA,* on day 6 PI when C57BL/6 displayed symptoms of ECM development. (*n* = 3-5 mice per group, unpaired, two tailed *t*-test; *$P \leq 0.05$. Data is representative of three independent experiments performed.

Figures

Figure 1. *IFNAR1* gene SNP alleles protect against malaria progression to cerebral malaria syndrome but confer increased susceptibility to malaria infection.

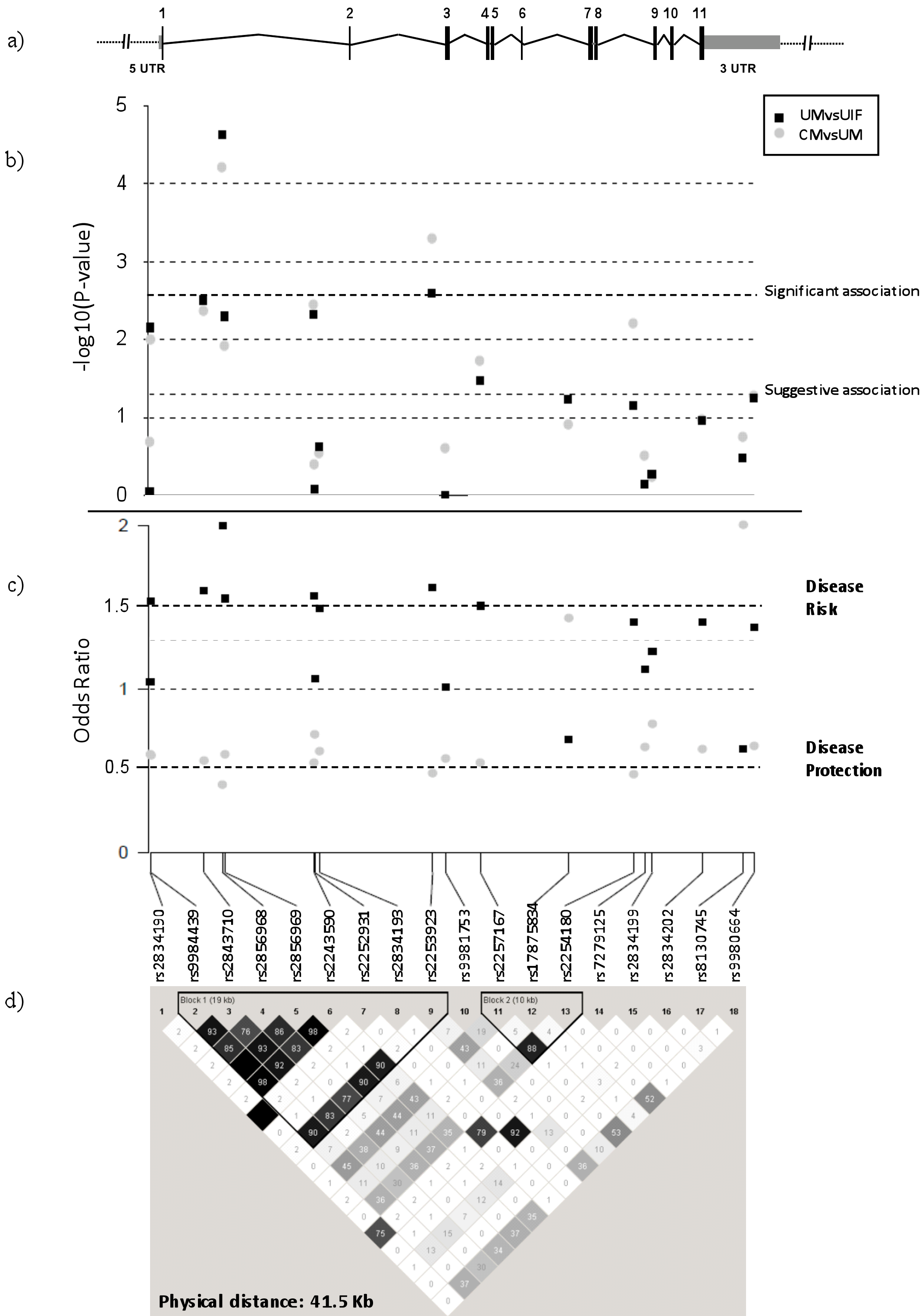

Figure 2. *Ifnar1-/-* mice are protected from ECM development and show no decrease in parasite burden.

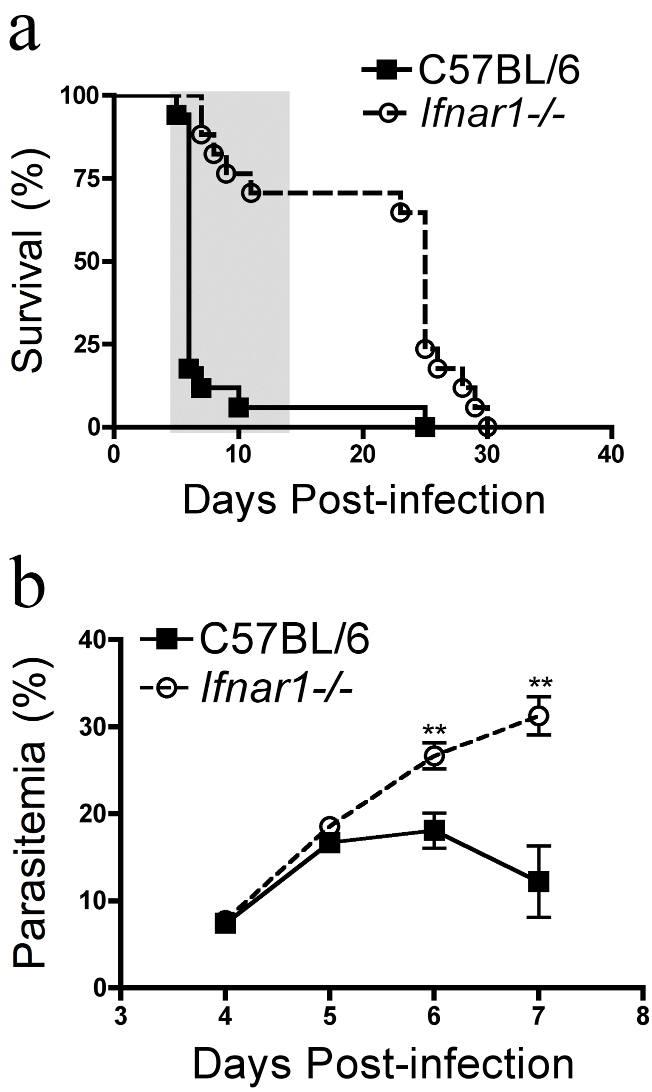

Figure 3. *Ifnar1-/-* mice are protected from BBB breakage and show reduced mononuclear cell accumulation in brain microvasculature.

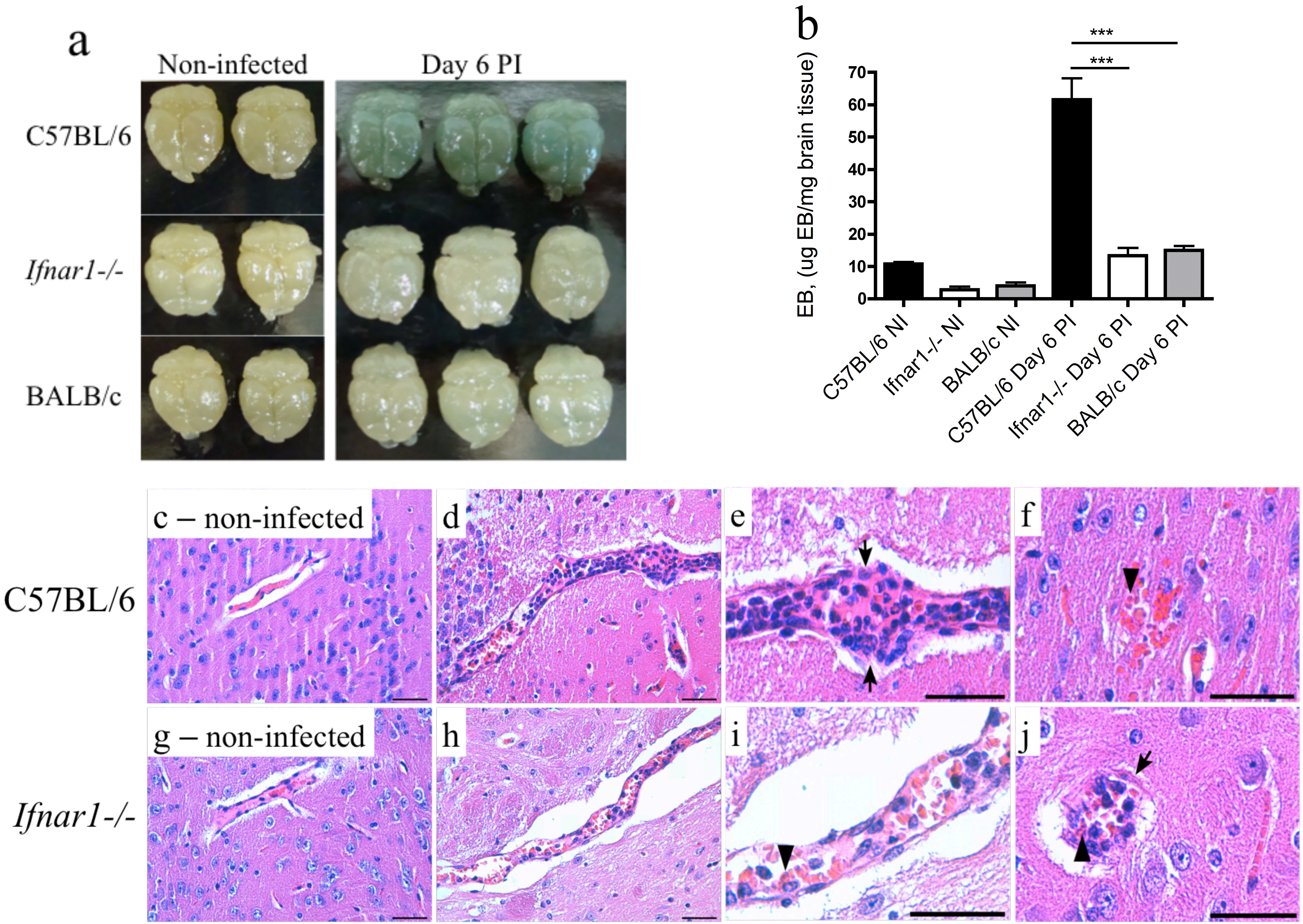

Figure 4. Parasite accumulation and brain inflammation markers in *Ifnar1-/-* infected mice.

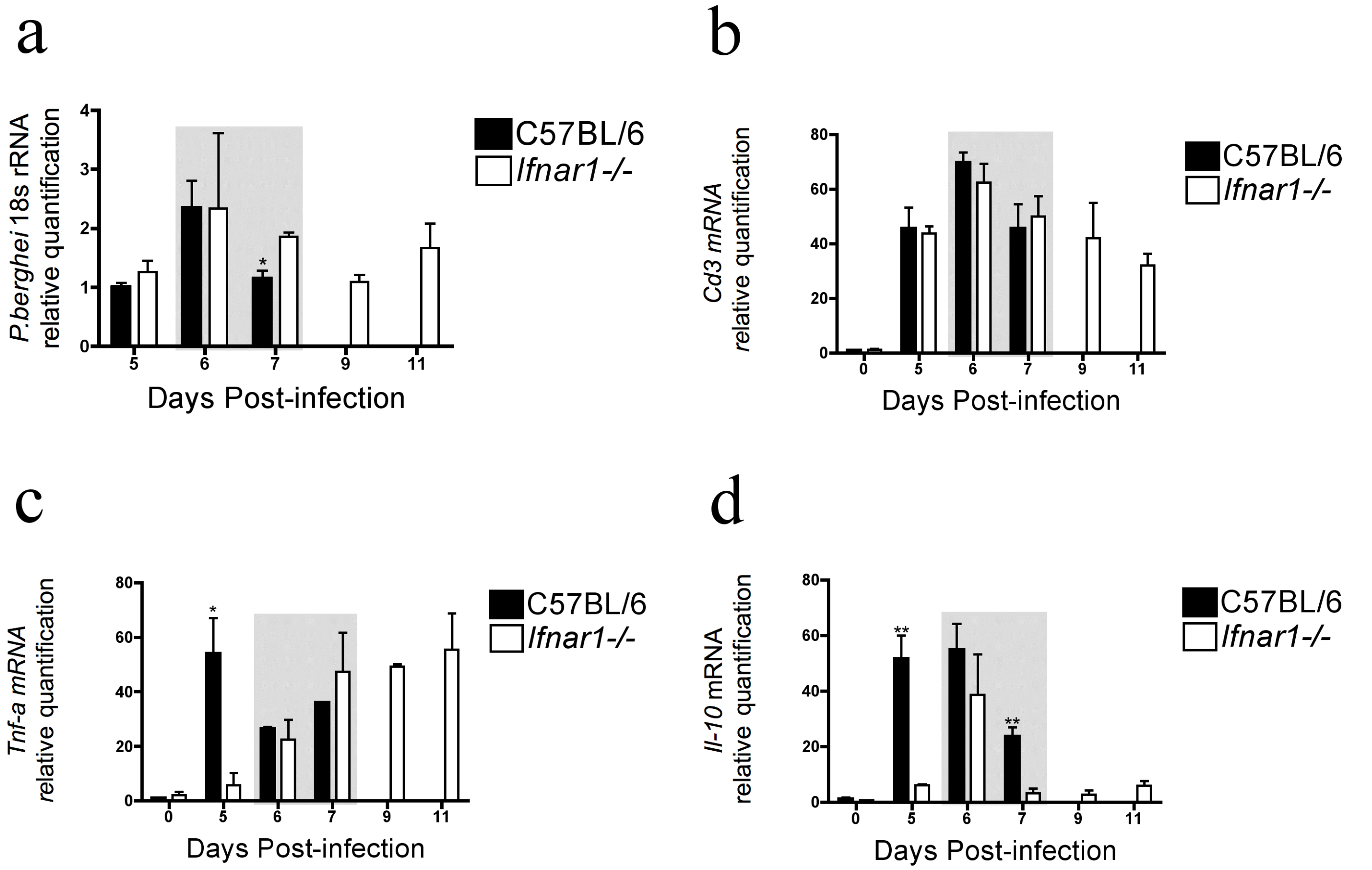

Figure 5. *Ifnar1-/-* mice succumb to ECM upon cell transfer of parasite sensitized splenocytes, explicitly $CD8^+$ cells.

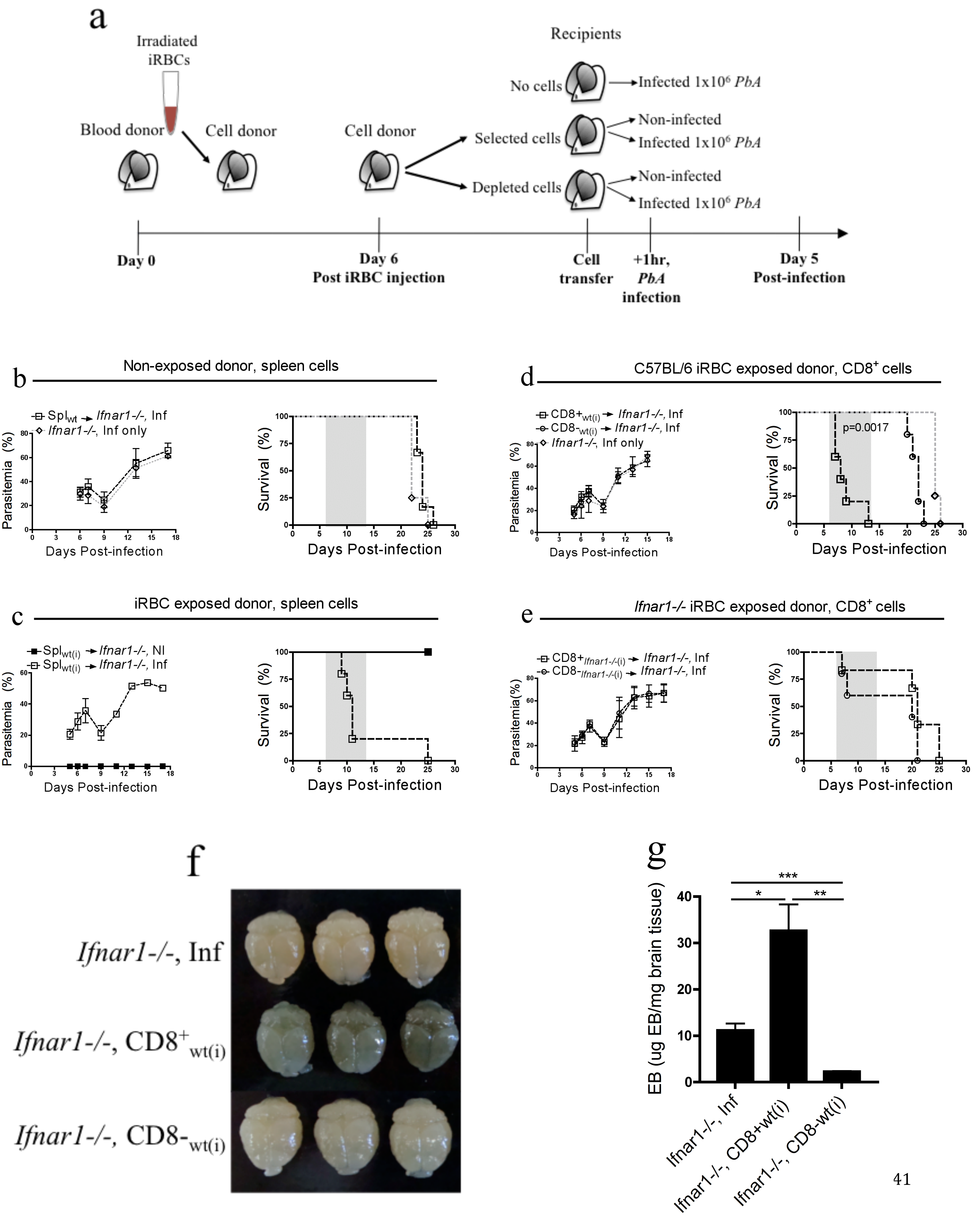

Figure 6. Intrinsic *Ifnar1-/-* $CD8^+$ cell impairment protects from ECM.

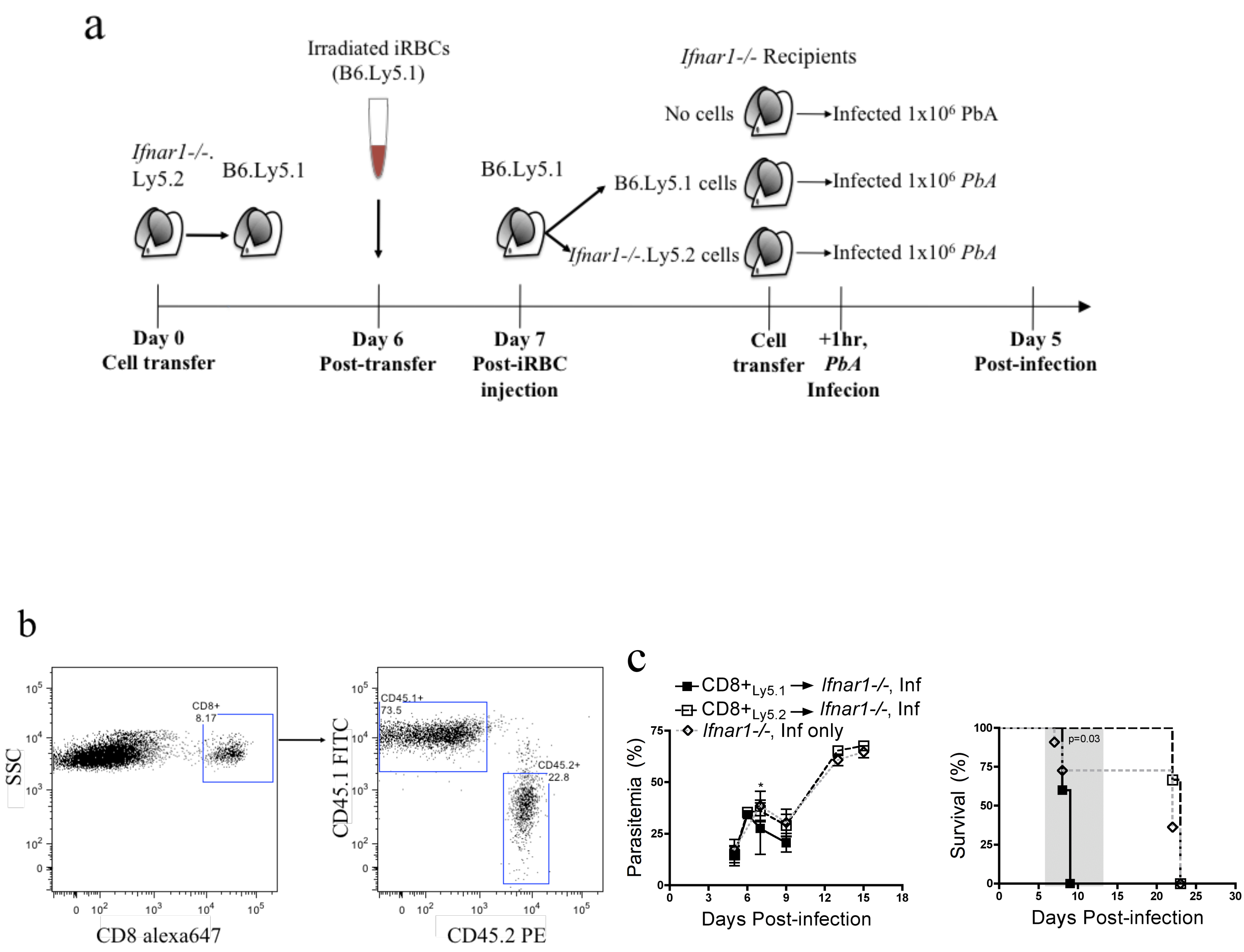

Figure 7. *Ifnar1-/-* $CD8^+$ T cell display activation phenotype upon *P.berghei* infection but do not accumulate in the brain.

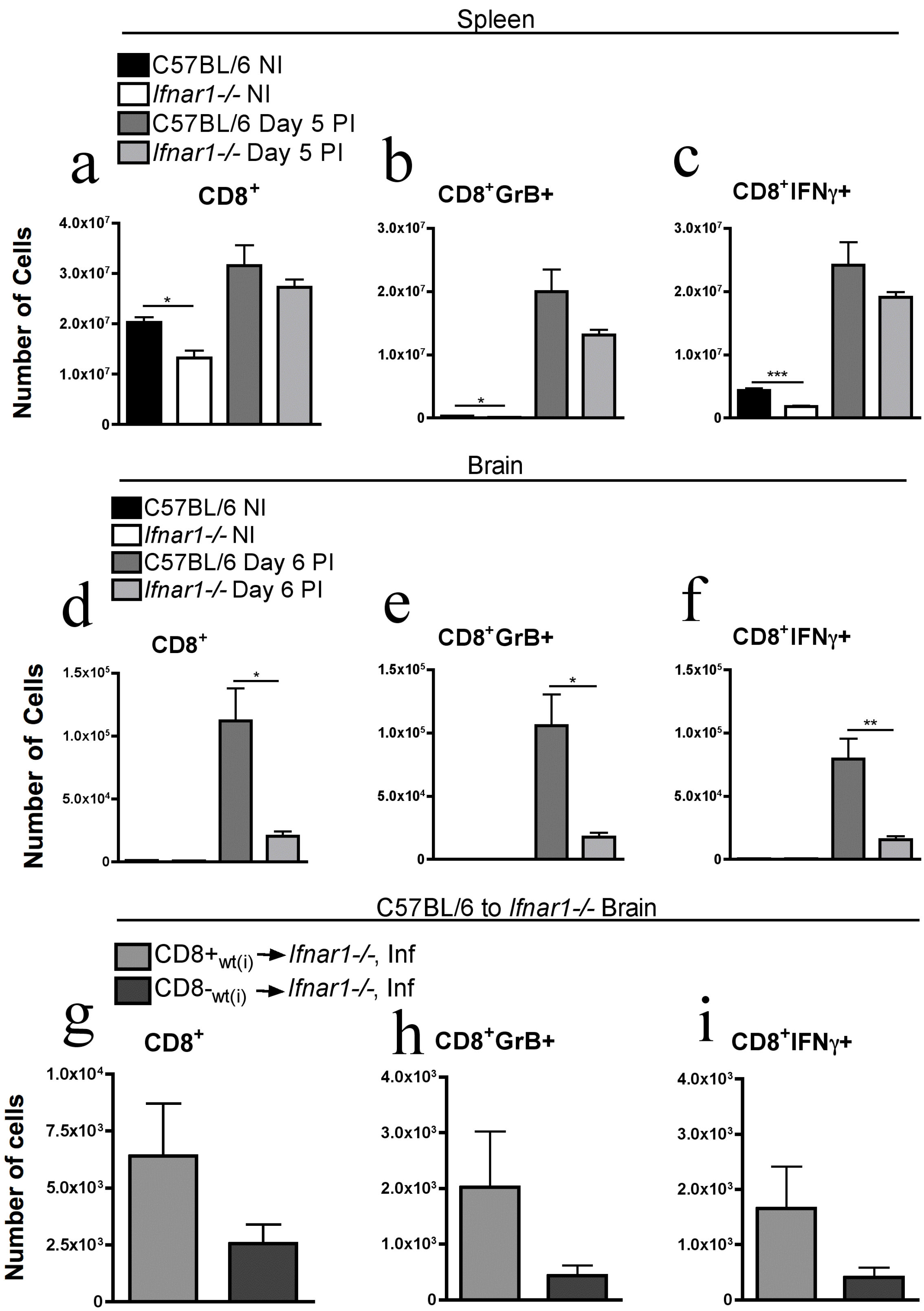

Tables

Table 1. *IFNAR1* haplotypes conferring susceptibility to uncomplicated malaria and protection against cerebral malaria.

Haplotypes	**Haplotype frequencies (%)**			**CM vs UM**		**UM vs UIF**	
	CM (2n = 220)	**UM (2n = 258)**	**UIF (2n = 610)**	***P*-value**	**OR (95% CI)**	***P*-value**	**OR(95% CI)**
Block 1							
GGGGTGCT	16.4	36.8	22.4	**6.89E-07**	0.34 (0.22-0.52)	**1.22E-05**	2.02 (1.47-2.77)
ACAACGCA	64.5	49.2	61.1	**8.00E-04**	1.87 (1.29-2.71)	**1.20E-03**	0.62 (0.46-0.83)
ACAACACA	4.3	5.5	6.4	0.5378	0.77 (0.33-1.79)	0.6827	0.88 (0.47-1.63)

In each haplotype are sequentially represented the alleles from SNPs of LD block 1 (rs9984439, rs2843710, rs2856968, rs2856969, rs2243590, rs2252931, rs2834193, rs2253923) as defined in Figure 1 (d). Significant *P*-values (<0.05) are highlighted in bold. Abbreviations: CM, cerebral malaria; UM, uncomplicated malaria; UIF, uninfected controls; OR, odds ratio; 95% CI, 95% confidence interval.

Supplemental Material

Figure S1. Transfer of $CD8^{+}$ cells from non-exposed donors, cannot induce ECM in *Ifnar1-/-* mice.

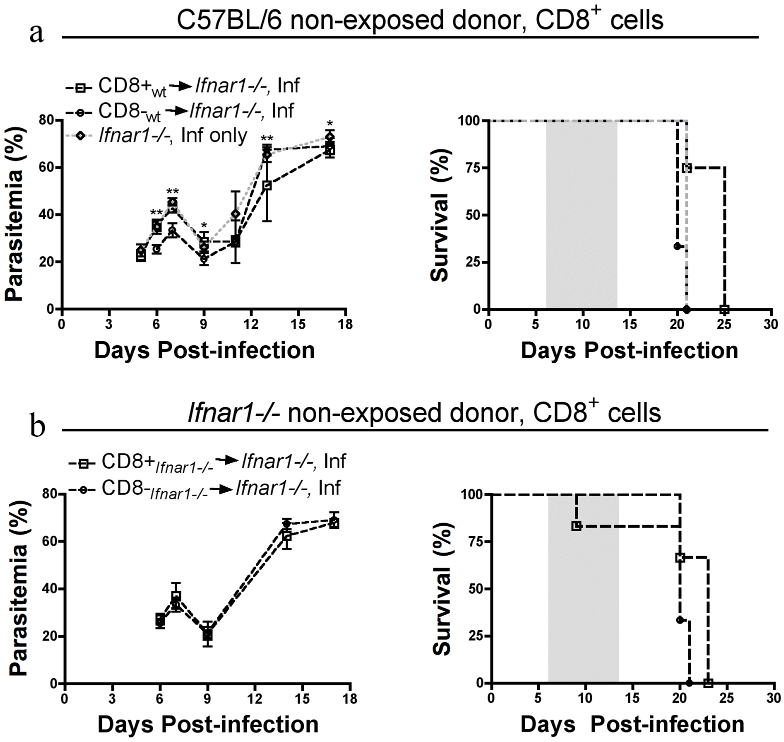

Figure S2. ECM induced *Ifnar1-/-* mice show no hindrance in cytotoxic expression ability compared to C57BL/6 mice.

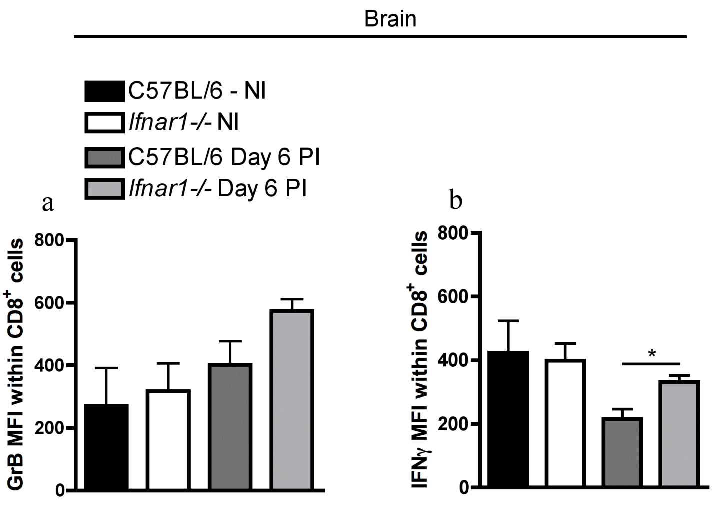

Supplemental Table 1. Collection dataset of Angolan children used for cerebral malaria and uncomplicated malaria case-control analyses (samples remaining after quality control).

Collection	***n***	**Mean age (months)**	**Male**	**Female**
CM	110	54.6	67	43
UM	129	49.1	69	60
UIF	305	61.5	171	133
Total	544		307	236

Abbreviations: CM, cerebral malaria; UM, uncomplicated malaria; UIF, uninfected controls; *n*, number of individuals.

Supplemental Table 2. Results of SNP allelic association in *IFNAR1* gene at 21q22.1 with cerebral malaria (CM vs UIF), with uncomplicated malaria (UM vs UIF) and with progression to cerebral malaria (CM vs UM).

						Assoc Allele numbers (frequency)			**CM vs UM**			**UM vs UIF**			**CM vs UIF**	
SNP ID	**SNP reference**	**Position (Mb)**	**Alleles[a]**	**Gene region**	**Assoc Allele**	**CM (2n = 220)**	**UM (2n = 258)**	**UIF (2n = 610)**	***P*-value**	**OR(95% CI)**	***P*-value$_{corr}$**	***P*-value**	**OR(95% CI)**	***P*-value$_{corr}$**	***P*-value**	**OR(95% CI)**
1	rs2834190	34693011	A/T	Promoter	T	10 (0.046)	19 (0.074)	43 (0.071)	0.2069	0.61 (0.28-1.33)	NS	0.8789	1.05 (0.60-1.83)	NS	0.1989	0.63 (0.31-1.28)
2	rs9984439	34693063	A/G	Promoter	G	57 (0.261)	94 (0.373)	166 (0.279)	**9.80E-03**	0.60 (0.40-0.88)	NS	**7.00E-03**	1.53 (1.12-2.10)	NS	0.6107	0.91 (0.64-1.30)
3	rs2843710	34696707	C/G	Promoter	G	55 (0.250)	96 (0.372)	162 (0.271)	**4.20E-03**	0.56 (0.38-0.84)	NS	**3.10E-03**	1.60 (1.17-2.18)	NS	0.5482	0.90 (0.63-1.28)
4	rs2856968	34697981	A/G	Intron 1	G	39 (0.197)	94 (0.370)	124 (0.227)	**6.15E-05**	0.42 (0.27-0.64)	**1.11E-03**	**2.36E-05**	2.00 (1.45-2.76)	**4.25E-04**	0.3798	0.84 (0.56-1.25)
5	rs2856969	34698159	A/G	Intron 1	G	57 (0.264)	96 (0.372)	165 (0.276)	**1.21E-02**	0.61 (0.41-0.90)	NS	**5.00E-03**	1.56 (1.14-2.12)	NS	0.7336	0.94 (0.66-1.34)
6	rs2243590	34704276	C/T	Intron 1	T	55 (0.257)	96 (0.384)	170 (0.285)	**3.60E-03**	0.56 (0.37-0.83)	NS	**4.80E-03**	1.56 (1.15-2.13)	NS	0.4291	0.87 (0.61-1.24)
7	rs2252931	34704320	A/G	Intron 1	A	12 (0.055)	19 (0.074)	42 (0.069)	0.3981	0.73 (0.34-1.53)	NS	0.8199	1.07 (0.61-1.87)	NS	0.4480	0.78 (0.40-1.50)
8	rs2834193	34704660	C/T	Intron 1	T	8 (0.037)	15 (0.058)	24 (0.040)	0.2869	0.62 (0.26-1.50)	NS	0.2338	1.49 (0.77-2.89)	NS	0.8605	0.93 (0.41-2.10)
9	rs2253923	34712419	A/T	Intron 2	T	48 (0.224)	96 (0.372)	163 (0.269)	**5.00E-04**	0.49 (0.32-0.73)	**9.00E-03**	**2.50E-03**	1.61 (1.18-2.20)	**4.50E-02**	0.1987	0.79 (0.54-1.14)
10	rs9981753	34713317	C/T	Exon 3	C	7 (0.032)	14 (0.055)	33 (0.054)	0.2422	0.58 (0.23-1.46)	NS	0.9721	1.01 (0.53-1.92)	NS	0.2019	0.59 (0.26-1.34)
11	rs2257167	34715699	C/G	Exon 4	C	28 (0.127)	53 (0.209)	89 (0.149)	**1.89E-02**	0.55 (0.34-0.91)	NS	**3.38E-02**	1.50 (1.03-2.19)	NS	0.4250	0.83 (0.53-1.31)
12	rs17875834	34721782	C/T	Exon 8	T	50 (0.227)	44 (0.171)	137 (0.228)	0.1199	1.43 (0.91-2.25)	NS	0.0571	0.70 (0.99-2.10)	NS	0.9744	0.99 (0.69-1.44)
13	rs2254180	34726230	C/T	Intron 10	C	22 (0.116)	55 (0.215)	96 (0.163)	**6.20E-03**	0.48 (0.28-0.82)	NS	0.0689	1.41 (0.97-2.04)	NS	0.1164	0.67 (0.41-1.11)
14	rs7279125	34727015	A/C	Intron 10	C	9 (0.041)	16 (0.062)	34 (0.056)	0.3016	0.65 (0.28-1.49)	NS	0.7167	1.12 (0.61-2.07)	NS	0.3949	0.72 (0.34-1.53)
15	rs2834199	34727516	A/G	Intron 10	A	10 (0.046)	15 (0.058)	29 (0.048)	0.5656	0.79 (0.35-1.79)	NS	0.5222	1.23 (0.65-2.34)	NS	0.9336	0.97 (0.46-2.02)
16	rs2834202	34730954	A/G	Exon 11	G	23 (0.105)	40 (0.155)	70 (0.115)	0.1038	0.64 (0.37-1.10)	NS	0.1068	1.41 (0.93-2.14)	NS	0.6700	0.90 (0.55-1.48)

17	rs8130745	34733770	C/T	Downstream	C	10 (0.045)	6 (0.023)	22 (0.037)	0.1787	2.00 (0.72-5.59)	NS	0.3289	0.64 (0.63-3.92)	NS	0.5352	1.27 (0.59-2.73)
18	rs9980664	34734510	A/C	Downstream	A	44 (0.220)	77 (0.301)	140 (0.238)	0.0525	0.66 (0.43-1.01)	NS	0.0554	1.38 (0.99-1.91)	NS	0.6013	0.90 (0.61-1.33)

Univariately significant *P*-values (<0.05) and significant Bonferroni corrected *P*-values (*P*-value$_{corr}$; <0.05) are highlighted in bold. Abbreviations: CM, cerebral malaria; UM, uncomplicated malaria; UIF, uninfected controls; Mb, Megabases; OR, odds ratio; 95% CI, 95% confidence interval; NS, not significant; a Major/minor allele; Assoc Allele, associated allele.

Supplemental Table 3. Results of SNP genotypic association in *IFNAR1* gene at 21q22.1 with cerebral malaria (CM vs UIF), uncomplicated (UM vs UIF) and with progression to cerebral malaria (CM vs UM).

						Genotype numbers (frequency %)			CM vs UM			UM vs UIF			CM vs UIF	
SNP ID	**SNP reference**	**Position (Mb)**	**Alleles[a]**	**Gene region**	**Genotypes**	**CM (n = 110)**	**UM (n = 129)**	**UIF (n = 305)**	***P*-value**	**OR(95% CI)**	***P*-value$_{corr}$**	***P*-value**	**OR(95% CI)**	***P*-value$_{corr}$**	***P*-value**	**OR(95% CI)**
1	rs2834190	34693011	A/T	Promoter	A/A	99 (90.8)	113 (87.6)	266 (87.5)	0.4238	0.71(0.31-1.64)	NS	0.9777	0.99(0.53-1.85)	NS	0.3421	0.71(0.34-1.47)
					T/A-T/T	10 (9.2)	16 (12.4)	38 (12.5)								
2	rs9984439	34693063	A/G	Promoter	A/A	60 (55.0)	48 (38.1)	150 (50.5)	**9.19E-03**	0.50(0.30-0.85)	NS	**1.88E-02**	1.66(1.08-2.54)	NS	0.4168	0.83(0.54-1.29)
					A/G-G/G	49 (45.0)	78 (61.9)	147 (49.5)								
3	rs2843710	34696707	C/G	Promoter	C/C	63 (57.3)	49 (38.0)	155 (51.8)	**2.83E-03**	0.46(0.27-0.77)	NS	**8.18E-03**	1.76(1.15-2.68)	NS	0.3280	0.80(0.52-1.25)
					C/G-G/G	47 (42.7)	80 (62.0)	144 (48.2)								
4	rs2856968	34697981	A/G	Intron 1	A/A	70 (70.7)	49 (38.6)	169 (61.9)	**1.22E-06**	0.26(0.15-0.46)	**2.20E-05**	**1.00E-05**	2.59(1.68-3.99)	**1.80E-04**	0.1138	0.67(0.41-1.11)
					G/A-G/G	29 (29.3)	78 (61.4)	104 (38.1)								
5	rs2856969	34698159	A/G	Intron 1	A/A	60 (55.6)	49 (38.0)	153 (51.2)	**6.77E-03**	0.49(0.29-0.82)	NS	**1.18E-02**	1.71(1.12-2.61)	NS	0.4338	0.84(0.54-1.30)
					A/G-G/G	48 (44.4)	80 (62.0)	146 (48.8)								
6	rs2243590	34704276	C/T	Intron 1	C/C	60 (56.1)	49 (39.2)	148 (49.7)	**1.01E-02**	0.51(0.30-0.85)	NS	**4.82E-02**	1.53(1.00-2.34)	NS	0.2546	0.77(0.50-1.21)
					C/T-T/T	47 (43.9)	76 (60.8)	150 (50.3)								
7	rs2252931	34704320	A/G	Intron 1	G/G	99 (90.0)	113 (87.6)	266 (87.8)	0.5573	0.78(0.35-1.77)	NS	0.9557	1.02(0.54-1.90)	NS	0.5297	0.80(0.39-1.63)
					A/G-A/A	11 (10.0)	16 (12.4)	37 (12.2)								
8	rs2834193	34704660	C/T	Intron 1	C/C	100 (92.6)	116 (89.9)	279 (92.4)	0.4687	0.71(0.28-1.79)	NS	0.4051	1.36(0.67-2.78)	NS	0.9438	0.97(0.42-2.24)

					C/T-T/T	8 (7.4)	13 (10.1)	23 (7.6)								
9	rs2253923	34712419	A/T	Intron 2	A/A	68 (63.6)	48 (37.2)	159 (52.5)	**5.00E-05**	0.34(0.20-0.58)	**9.00E-04**	**3.50E-03**	1.86(1.22-2.84)	NS	**4.63E-02**	0.63(0.40-1.00)
					T/A-T/T	39 (36.4)	81 (62.8)	144 (47.5)								
10	rs9981753	34713317	C/T	Exon 3	T/T	101 (93.5)	114 (89.1)	275 (90.2)	NA	NA	NA	0.7309	1.13(0.58-2.20)	NS	0.2791	0.64(0.27-1.49)
					T/C-C/C	-----	14 (10.9)	30 (9.8)								
11	rs2257167	34715699	C/G	Exon 4	G/G	83 (75.5)	80 (63.0)	214 (71.8)	**3.79E-02**	0.55(0.31-0.97)	NS	0.0740	1.50(0.96-2.32)	NS	0.4601	0.83(0.50-1.37)
					G/C-C/C	27 (24.5)	47 (37.0)	84 (28.2)								
12	rs17875834	34721782	C/T	Exon 8	C/C	69 (62.7)	87 (67.4)	173 (57.7)	0.4457	1.23(0.72-2.10)	NS	0.0556	0.66(0.43-1.01)	NS	0.3543	0.81(0.52-1.27)
					T/C-T/T	41 (37.3)	42 (32.6)	127 (42.3)								
13	rs2254180	34726230	C/T	Intron 10	T/T	74 (77.9)	82 (64.1)	213 (72.2)	**2.44E-02**	0.51(0.28-0.93)	NS	0.0969	1.46(0.94-2.27)	NS	0.2675	0.74(0.43-1.27)
					C/T-C/C	21 (22.1)	46 (35.9)	82 (27.8)								
14	rs7279125	34727015	A/C	Intron 10	A/A	101 (91.8)	116 (89.9)	275 (90.2)	0.6122	0.80(0.33-1.94)	NS	0.9388	1.03(0.52-2.04)	NS	0.6055	0.82(0.37-1.78)
					C/A-C/C	9 (8.2)	13 (10.1)	30 (9.8)								
15	rs2834199	34727516	A/G	Intron 10	G/G	99 (91.7)	116 (89.9)	276 (90.8)	0.6439	0.81(0.33-1.98)	NS	0.7792	1.10(0.55-2.21)	NS	0.7826	0.90(0.41-1.97)
					A/G-A/A	9 (8.3)	13 (10.1)	28 (9.2)								
16	rs2834202	34730954	A/G	Exon 11	A/A	90 (81.8)	91 (70.5)	241 (79.3)	**4.11E-02**	0.53(0.29-0.98)	NS	0.0528	1.60(1.00-2.55)	NS	0.5652	0.85(0.49-1.49)
					G/A-G/G	20 (18.2)	38 (29.5)	63 (20.7)								
17	rs8130745	34733770	C/T	Downstream	T/T	102 (92.7)	123 (95.3)	284 (93.1)	0.3905	1.61(0.54-4.78)	NS	0.3659	0.66(0.26-1.67)	NS	0.8917	1.06(0.46-2.47)
					C/T-C/C	8 (7.3)	6 (4.7)	21 (6.9)								
18	rs9980664	34734510	A/C	Downstream	C/C	64 (64.0)	64 (50.0)	178 (60.5)	0.0339	0.56(0.33-0.96)	NS	0.0447	1.53(1.01-2.33)	NS	0.5385	0.86(0.54-1.38)
					C/A-A/A	36 (36.0)	64 (50.0)	116 (39.5)								

The genetic association *P*-values are under the dominant model. Numbers of genotypes are givenalong with percentages within each group (CM, UM, UIF) within parentheses. Univariately significant *P*-values (<0.05) and significant Bonferroni corrected p-values (*P*-valuecorr; <0.05) are highlighted in bold. Abbreviations: CM, cerebral malaria; UM, uncomplicated malaria; UIF, uninfected controls; Mb, Megabases; OR, odds ratio; 95% CI, 95% confidence interval; NA, not available; NS, not significant; a Major/minor allele.